SCIPP-92-10

SCIPP 92/10
March 1992

Fermilab Library
0 1160 0013259 1

41

Higgs Theory and Phenomenology at Future e^+e^- Linear Colliders*

HOWARD E. HABER
Santa Cruz Institute for Particle Physics
University of California, Santa Cruz, CA 95064

Abstract

The theory of Higgs bosons and its application to the Higgs search at future e^+e^- linear colliders is reviewed. Both the minimal Higgs model and nonminimal extensions are considered. Particular attention is given to the Higgs sector of the minimal supersymmetric model (MSSM). If radiative corrections are included, it appears very possible that all Higgs bosons of the MSSM are beyond the kinematic reach of LEP and LEP-II. As a result, the next linear collider (NLC) may be indispensable in unraveling the detailed properties of the Higgs boson.

JUN 1 1992
SLAC LIBRARY

Submitted to:
Proceedings of the Workshop on Future e^+e^- Linear Colliders
Saariselkä, Finland, September 9–14, 1991

RETURN TO SLAC LIBRARY
FILMED
DATE
DOCUMENT
LOCATION

* Work supported in part by the U.S. Department of Energy.

Higgs Theory and Phenomenology at Future e^+e^- Linear Colliders

HOWARD E. HABER
Santa Cruz Institute for Particle Physics
University of California, Santa Cruz, CA 95064, U.S.A.

Abstract

The theory of Higgs bosons and its application to the Higgs search at future e^+e^- linear colliders is reviewed. Both the minimal Higgs model and nonminimal extensions are considered. Particular attention is given to the Higgs sector of the minimal supersymmetric model (MSSM). If radiative corrections are included, it appears very possible that all Higgs bosons of the MSSM are beyond the kinematic reach of LEP and LEP-II. As a result, the next linear collider (NLC) may be indispensable in unraveling the detailed properties of the Higgs boson.

1. Introduction: The Higgs Hunter's Flow Chart

After two years of running at LEP and over a million Z^0 events accumulated, the Standard Model of particle physics continues to provide a detailed and complete description of all observed high energy physics phenomena. Yet, the final chapter of the Standard Model is not yet written. The top quark remains to be discovered; present limits from the CDF Collaboration imply $m_t > 91$ GeV.[1] Moreover, the data from LEP already places nontrivial constraints on the upper limit of the top-quark mass, based on the precision measurements of various electroweak observables, which depend on the top-quark mass when radiative corrections (due to virtual top-quark exchange) are taken into account.[2,3] The final element of the Standard Model which remains to be uncovered is the mechanism for electroweak symmetry breaking. The central goal of particle physics in the 1990s and beyond is to uncover and elucidate the mechanism for W and Z (and fermion) mass generation by conducting experiments that can probe the energy scale between 100 GeV and 1 TeV. Furthermore, there are a number of theoretical arguments that strongly suggest that this endeavor will also lead to the first hints of deviations from the Standard Model.[4] That is, the exploration of the origins of electroweak symmetry breaking may reveal new phenomena with far reaching implications for future theories of particle physics.

At the present time, we are remarkably ignorant as to the detailed mechanism of electroweak symmetry breaking. The Standard Model posits the existence of one complex doublet of elementary scalars. When the neutral component of this doublet acquires a vacuum expectation value, mass is generated for the $W^\pm$ and Z guage bosons (as well as for the quarks and charged leptons). The other physical remnant of this mechanism is the existence of one CP-even scalar Higgs boson. However, numerous other scenarios exist. The scalar sector can be enlarged in a number of ways without running into conflict with present experimental knowledge. For example, the physical Higgs sector can contain charged scalars and additional CP-even and CP-odd neutral scalars. In other approaches, the elementary scalar sector is removed entirely and replaced by new fermions and new forces. The dynamics of these new forces is invoked to break the electroweak symmetry breaking. Scalar states can arise in such models, although such states would be composites of more fundamental entities. Technicolor models are theories of this type.[5]

The minimal Higgs model, which contains exactly one physical CP-even scalar, provides a convenient benchmark for designing experiments at future colliders to probe the electroweak symmetry breaking sector. However, such a theory with fundamental elementary scalars is problematical. If the electroweak model is embedded in a more fundamental structure characterized by a much larger energy scale (*e.g.*, the Planck scale, which must appear in any theory including gravity), the Higgs boson would tend to acquire mass of order the largest energy scale due to radiative corrections. Only by adjusting (*i.e.*, "fine-tuning") the parameters of the Higgs potential "unnaturally" can one arrange a large hierarchy between the Planck scale and the scale of electroweak symmetry breaking.[4,6] The Standard Model provides no mechanism for this. Various proposals to solve this "hierarchy" problem have been advanced in the literature. Two examples are technicolor models and supersymmetric models. In a supersymmetric theory the radiative corrections to scalar masses are controlled by the cancellation of contributions from particles and their supersymmetric partners. Since supersymmetry cannot be an exact symmetry of nature, the cancellation must be incomplete, and the Higgs mass receives contributions that are limited by the extent of the supersymmetry breaking. In order that the naturalness and hierarchy problems be resolved, it is necessary that the scale of supersymmetry breaking not exceed $\mathcal{O}(1\text{ TeV})$.[7] Such "low-energy" supersymmetric theories are especially interesting in that, to date, they provide the only theoretical framework in which the problems of naturalness and hierarchy can be resolved while retaining the Higgs bosons as truly elementary spin-0 particles.

The primary mission of the next generation of high energy supercolliders is to identify the underlying physics that is responsible for the generation of the electroweak symmetry breaking scale. The Higgs mechanism describes how the W and

Z acquire their masses and low-energy couplings by the absorption ("eating") of Goldstone bosons that have been generated by some symmetry breaking mechanism. With the discovery of the W and Z bosons and the confirmation of their Standard Model properties, the Higgs mechanism has been essentially verified, but the dynamics that generates the Goldstone bosons remains unknown.[8] In the Standard Model, it is the dynamics of the scalar Higgs sector that is responsible for electroweak symmetry breaking. In alternative approaches, one can often identify physical states that replace or resemble the Higgs bosons. Thus, the search for the Higgs boson takes center stage in the physics programs of all future supercolliders. Beyond the Higgs bosons (or equivalents) one hopes to expose the underlying physics of the TeV scale responsible for the electroweak symmetry breaking dynamics. Thus, an equally important aspect of experiments at future supercolliders involves the search for new physics beyond the Standard Model. As in the case of low-energy supersymmetry, these two aspects are often intimately tied together.

As emphasized above, there is at present no experimental information that provides any clue as to the nature of the physics that generates electroweak symmetry breaking. Therefore, in planning for the physics programs at future supercolliders, one must allow for a plethora of possibilities. In order to organize the variety of possible paths in a coherent fashion, I have put together a flow chart in fig. 1 to indicate the necessary steps for constructing a theoretical model of electroweak symmetry breaking. Clearly, a comprehensive tour through this chart would require a book.[9] In this paper, I will only have the opportunity to explore a few of the available avenues. Nevertheless, let us take a brief tour to see what the various possibilities are.

The first question a Higgs Hunter must decide is whether the Higgs bosons are elementary or composite. The Standard Model makes use of elementary Higgs bosons. However, for the reasons indicated above, one expects the physics responsible for electroweak symmetry breaking to lie beyond the Standard Model. Models of low-energy supersymmetry provide the most compelling framework for elementary Higgs bosons, and these models have been widely studied in recent times.[9–12] It is generally thought that elementary Higgs bosons must be weakly coupled.[13] In the Standard Model, the strength of the Higgs self-coupling is proportional to the square of its mass. Upper limits to the Higgs mass from lattice analyses argue against the possibility of a strongly coupled elementary Higgs boson.[14,15] In the case of composite Higgs bosons, scalar particles are bound states of more fundamental constituents (usually fermions which carry a new strong interaction quantum number such as technicolor). Strongly interacting systems are difficult to analyze, and various theoretical techniques (such as chiral Lagrangians) have been used to explore the consequences of such theories.[16–18] Clearly, weakly interacting Higgs bosons, whose properties can be determined by perturbative techniques,

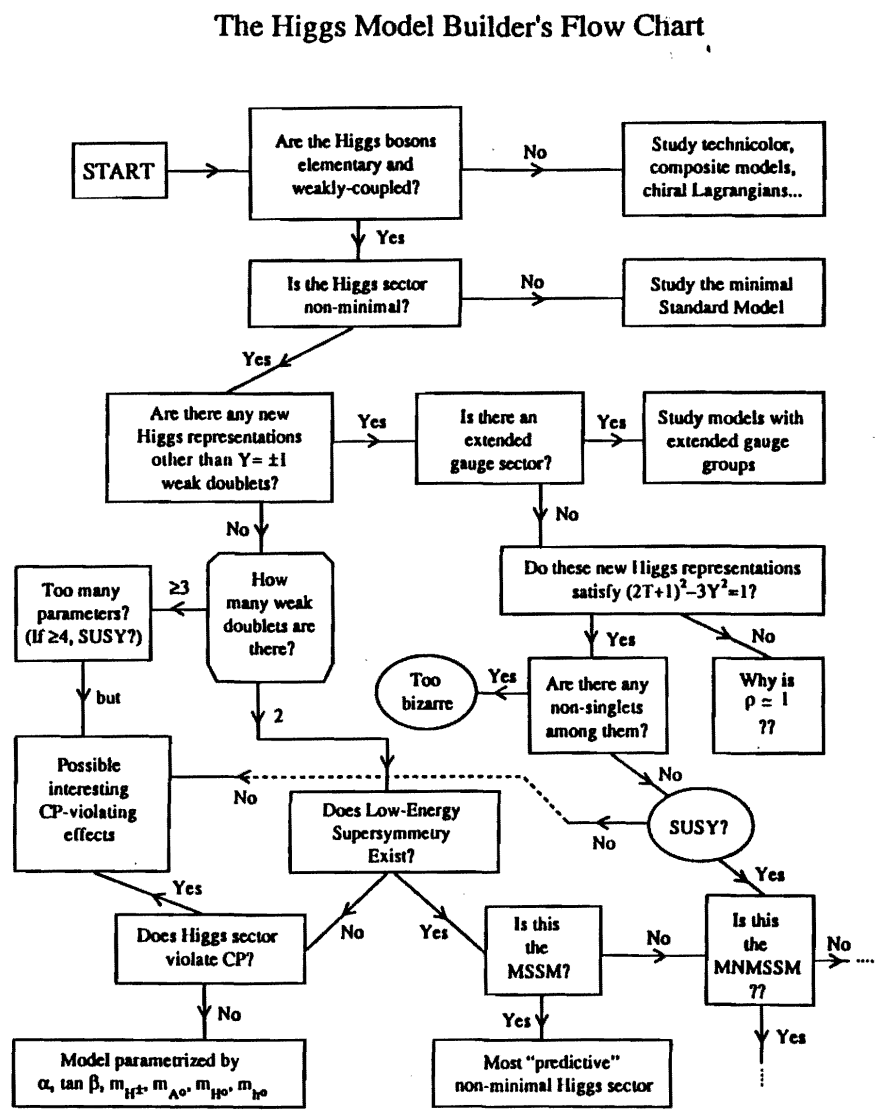

Fig. 1. The Higgs Hunter's Flow Chart.

provide a more specific phenomenology for future supercolliders. Thus, I will focus on such theories in this presentation.

Assuming Higgs bosons are elementary, one must decide if the Higgs sector is minimal or nonminimal. In the Standard Model, the Higgs sector consists of one scalar hypercharge-one weak doublet. The phenomenology of this Standard Model Higgs boson is the subject of section 2. Much of this phenomenology is also applicable, in part, to the case of the nonminimal Higgs sector. In the nonminimal case, a number of choices must be made. Should one expand the electroweak gauge sector as well? Perhaps—this is one of the questions that can only be answered by the next generation of supercolliders. I will not take this path here. What is the structure of the Higgs multiplets of the nonminimal Higgs sector? Does one simply duplicate the Standard Model Higgs doublet, or are there other types of multiplets? In the latter case, one must choose the new multiplets carefully to avoid spoiling the prediction: $\rho = m_W^2/(m_Z^2 \cos^2\theta_W) = 1$.[19,20] There are a number of ways to do this, but they are either ugly, unnatural and/or too bizarre. One can always safely add Higgs singlets. This is done by model builders in some nonminimal supersymmetric approaches or in models with CP-violating Higgs sectors. Adding such states does not usually have much impact on the phenomenology of Higgs bosons at supercolliders, and I shall avoid doing so here. Having made all the above choices, one is left with the task of exploring models with multi-Higgs doublets.

In the minimal Higgs model, there is one physical Higgs boson—a neutral CP-even scalar. In multi-Higgs doublet models, the scalar spectrum includes CP-even and CP-odd neutral Higgs scalars (assuming the Higgs sector conserves CP; otherwise states with opposite CP can mix) and charged Higgs scalars. Thus, extended Higgs sectors can increase considerably the richness of the Higgs phenomenology. All these states are present in a two Higgs doublet model—the simplest example of a multi-doublet model. The question of CP conservation mentioned above is an interesting one. Normally, there is no reason to expect multi-Higgs doublet models to conserve CP.[21] However, it is common practice to invoke such an assumption in order to simplify the phenomenological analysis. It is certainly worthwhile to contemplate how CP-violating effects could be detected in the Higgs sector at a supercollider; although I suspect that this will be difficult. Thus, in the study of multi-Higgs phenomenology at future supercolliders, an initial assumption of CP-conservation seems appropriate. The phenomenology of the CP-conserving two-Higgs-doublet model depends on six Higgs sector parameters and is the subject of section 3.

The Flow Chart then leads us to the question of supersymmetry. The minimal supersymmetric extension of the Standard Model (MSSM) consists of taking the Standard Model as it is known today (including the as yet undiscovered t-quark) and adding the corresponding supersymmetric partners.[22] In addition, the MSSM

contains two Higgs doublets, which is the minimal structure for the Higgs sector of a supersymmetric extension of the Standard Model that generates mass for both "up"-type and "down"-type quarks (and charged leptons). In particular, the MSSM Higgs sector is a CP-conserving two-Higgs-doublet model, which can be parametrized in terms of only two Higgs sector parameters (due to extra constraints imposed by supersymmetry). Thus the MSSM Higgs sector is the most predictive of the nonminimal Higgs models. Its phenomenology is the subject of section 4. In addition, one can consider nonminimal supersymmetric models. For example, the minimal nonminimal supersymmetric model (MNMSSM)[23] adds a complex Higgs singlet, and so on. The phenomenology becomes less constrained, and I will not pursue this path here.

If we are truly fortunate, the Higgs boson will soon be discovered either at LEP or LEP-II. However, for Higgs bosons heavier than the Z, the discovery and the exploration of Higgs physics must await the next generation of supercolliders. Both the hadron supercolliders (LHC and SSC) and the e^+e^- supercolliders (NLC and beyond) will be able to probe the Higgs landscape. One expects that the hadron supercolliders will have the first opportunity to make the initial Higgs boson discovery. How many Higgs states these machines can uncover if more than one is present is widely debated. Moreover, in some cases it will be difficult to ascertain more than the mere existence of a state with Higgs-like characteristics. In contrast, the e^+e^- supercolliders should be able to provide unambiguous detailed information on Higgs boson properties, and thus will play a crucial role in unraveling the mysteries of the origin of electroweak symmetry breaking. In this presentation, I shall review the body of work that has begun to explore how best to utilize future e^+e^- supercolliders in the pursuit of the Higgs boson. Some of this work was presented at parallel sessions at this meeting. A variety of energies have been proposed for future e^+e^- supercolliders. For convenience, I will use the following notation in what follows. The next linear collider, the NLC is assumed to have a center-of-mass energy between 300 and 500 GeV. An upgraded version of this machine, running at $\sqrt{s} = 1$ TeV will be referred to as the TLC.[24] Finally, there has been some studies at CERN of the physics potential at a 2 TeV linear collider called CLIC.[25] I will use this nomenclature simply to indicate the energy of the corresponding linear collider.

2. In Search of the Minimal Higgs Boson

The Standard Model predicts the existence of a single neutral CP-even Higgs scalar (called ϕ^0) with very specific properties. The tree-level couplings of ϕ^0 to

vector bosons and fermions are given by:

$$g_{\phi^0 VV} = g_V m_V \,, \qquad g_{\phi^0 f\bar{f}} = \frac{g m_f}{2 m_W} \,, \tag{1}$$

where $g_V = g\ [g/\cos\theta_W]$ for $V = W\ [Z]$. The Higgs mass is not predicted by the Standard Model, although consistency of the Standard Model as an effective low-energy theory requires $m_{\phi^0} \lesssim 800$ GeV.* Present limits on the Higgs mass from LEP are based on the nonobservation of $Z \to \phi^0 f\bar{f}$ [fig. 2(a)], where f represents all kinematically accessible quarks and leptons. Typical 95% CL limits are: $m_{\phi^0} > 51$ GeV, quoted by the ALEPH and OPAL collaborations; averaging over the four LEP experiments yields: $m_{\phi^0} > 58$ GeV.[27,28] As more Z data is accumulated, this limit will improve somewhat, with an eventual sensitivity around 65 GeV. To improve the Higgs mass limit further, one must upgrade LEP to higher energies. LEP-II, running at $\sqrt{s} > 2m_W$ will search for $e^+e^- \to \phi^0 Z$ [fig. 2(b)]. The eventual Higgs mass limit attainable at LEP-II lies between 80 and 95 GeV.[29] In order to reach the upper end of this mass range, one must be able to detect the $\phi^0 Z$ final state above the Standard Model $e^+e^- \to ZZ$ background.[30] This will require maximal energy ($\sqrt{s}$ near 200 GeV) and luminosity (more than 500 pb^{-1} of data), and a vertex detector with efficient b-tagging.

After LEP-II completes its Higgs search, one must await the supercollider era. Presumably, the hadron supercolliders (LHC and SSC) will turn on first, so I shall very briefly summarize the Higgs search capabilities of these machines.[9,31–33] For the sake of brevity, I will quote the expected range of Higgs masses accessible to the SSC running at $\sqrt{s} = 40$ TeV with an integrated luminosity (per year) of 10 fb^{-1}. The mass reach of the LHC is somewhat less, since its energy is lower; although it can improve its Higgs mass reach by increasing its luminosity. The "gold-plated" signature is the inclusive production of the Higgs boson followed by $\phi^0 \to ZZ \to \ell^+\ell^-\ell^+\ell^-$ (where $\ell = e$ or μ). Higgs bosons with a mass in the range $130 \lesssim m_{\phi^0} \lesssim 800$ GeV could be discovered at the SSC in its gold-plated mode. (Note that for $m_{\phi^0} < 2m_Z$, one of the two Z's is virtual; nevertheless the gold-plated rate is still sufficient in the mass range indicated.) The range of Higgs masses above 800 GeV is sometimes referred to as the "obese Higgs mass regime". As remarked above, it is very unlikely that a Higgs mass this heavy could

* This very rough estimate is obtained by lattice techniques and renormalization group analyses.[15,26] By adding additional theoretical assumptions, this upper limit can be reduced substantially. For example, by requiring that the Higgs and top-quark Yukawa couplings remain perturbative all the way up to the grand unification scale, one finds that $m_{\phi^0} \lesssim 200$ GeV.[13,26]

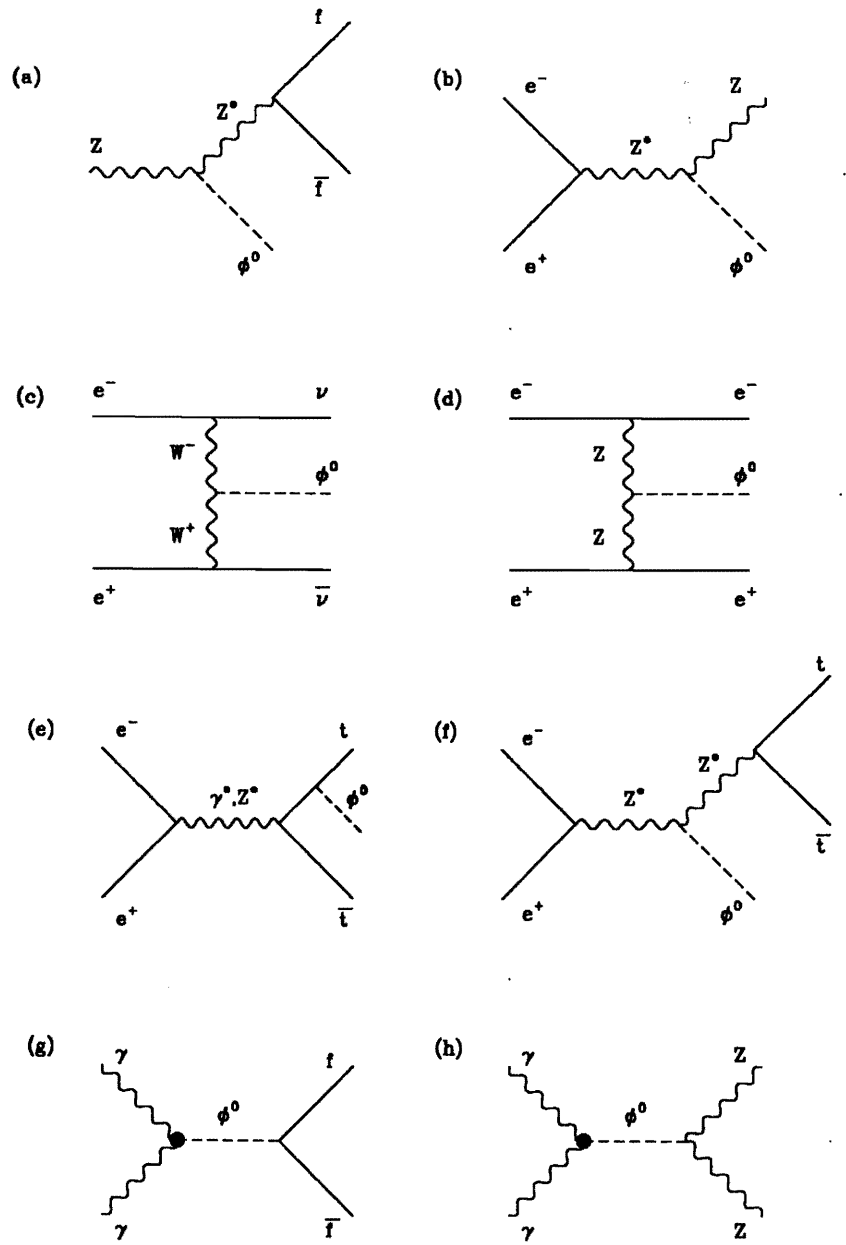

Fig. 2. Higgs production mechanisms at e^+e^- linear colliders from LEP to NLC and beyond. In (g) and (h) the incoming photons can be produced in a $\gamma\gamma$ collider mode via Compton backscattering of laser photons off linac electrons. The solid circle indicates that the $\gamma\gamma\phi^0$ coupling is induced at one-loop.

be consistent with a low-energy effective theory containing nothing more than the Standard Model. On the other hand, if no evidence for a Higgs boson with mass below 800 GeV is obtained, one would presumably expect a marked deviation from Standard Model predictions near 1 TeV. The new physics would likely be strongly interacting, so it is very hard to know exactly what to expect. There has been some theoretical and phenomenological efforts in this direction, and the interested reader can consult refs. 16 and 17 for further discussions of the strongly interacting electroweak symmetry breaking sector.

The range of Higgs masses between m_W and $2m_Z$ is called the "intermediate mass regime". Higgs bosons in the lower part of this range ($m_{\phi^0} \lesssim 130$ GeV) present a formidable challenge to the SSC and LHC. In order to detect a Higgs boson with a mass in this range, a variety of techniques have been proposed[34] including: (i) $gg \to \phi^0 \to \gamma\gamma$, (ii) $gg \to t\bar{t}\phi^0$, where the associated t-production (identified via a hard semileptonic decay) is used as a trigger, (iii) $q\bar{q} \to W^* \to W\phi^0$, and (iv) $gg \to \phi^0 \to \tau^+\tau^-$. In mechanisms (ii) and (iii), it has been suggested that the rare decay $\phi^0 \to \gamma\gamma$ may provide the cleanest signature for the intermediate mass Higgs boson. The proponents of these techniques are confident that an intermediate mass Higgs boson can be discovered at the SSC.[32–34] However, to isolate a signal, one must make severe cuts on the data to eliminate background. The final data sample after cuts often contains no more than a few tens of events. Thus, even if a Higgs signal is seen, it will be a challenge to unambiguously identify it as such. Moreover, little will be known about the properties of such a Higgs boson.

Based on the above discussion, it is very likely that the existence of the Higgs boson will have already been settled by the hadron supercolliders before the first e^+e^- supercollider (NLC) begins operations. Thus, one must carefully consider what the goals should be for an NLC intent on exploring Higgs physics. First, it should be emphasized that the intermediate mass Higgs boson presents no serious problems for the NLC. In fact, the NLC with $\sqrt{s}$ as low as 300 GeV (and 5 fb^{-1} luminosity) would be able to discover or rule out a Higgs boson with $m_{\phi^0} < 2m_Z$. This would settle definitively the question of the existence of an intermediate mass Higgs boson, if the results from the LHC and/or SSC were ambiguous. Once the Higgs boson mass is known (and assuming it lies within the energy reach of the NLC), experiments at the NLC will be able to measure a number of key Higgs properties—its spin, electroweak quantum numbers and the Higgs couplings to ZZ and heavy fermion pairs. In addition, one may have the capability of running the NLC in a $\gamma\gamma$ collision mode via Compton backscattering of laser photons off the linear collider electrons (and positrons).[35,36] The Higgs boson produced in such collisions would provide an accurate measurement of the $\phi^0\gamma\gamma$ coupling. This coupling is induced at the one-loop level and receives contributions from all virtual charged particles that get mass via the Higgs mechanism. Thus, the

measurement of the $\phi^0\gamma\gamma$ coupling would provide significant information on the mass generation mechanism of the Standard Model. At e^+e^- supercolliders of even higher energy and luminosity, the range of accessible Higgs masses clearly increases. Presumably, Higgs bosons in this mass range have already been cleanly identified at the LHC and SSC via the gold-plated mode. Nevertheless, the NLC (and TLC) still have a number of important tasks. The measurement of $\phi^0 \to t\bar{t}$ is crucial for the understanding of the fermion mass generation mechanism.* Other detailed properties of the Higgs boson must be obtained to check thoroughly the tree-level Higgs predictions of the Standard Model or the theory that supersedes it. With sufficient integrated luminosity, it may be possible via precision electroweak measurements to probe the one-loop radiative corrections to Higgs production and decay processes. Finally, at CLIC, sensitivity to the obese Higgs mass regime may present the cleanest environment for the study of physics at the 1 TeV mass scale.

Let us now take a brief tour of Higgs boson physics at the NLC. First, consider the various Higgs production mechanisms shown in fig. 2. At the NLC, the Higgs search at LEP-II could be extended over the entire intermediate mass Higgs regime via $e^+e^- \to \phi^0 Z$. The total cross sections for this process are shown in fig. 3 for $m_{\phi^0} = 100$ GeV as a function of the center-of-mass energy and in fig. 4 at $\sqrt{s} = 500$ GeV as a function of m_{ϕ^0}. These results were presented by B. Mele in the parallel sessions, based in part on the work of ref. 37. Complementary results can be found in refs. 38 and 39. This is one case where the lower energy ($\sqrt{s} = 300$ GeV) NLC has an advantage over a higher energy ($\sqrt{s} = 500$ GeV) NLC. At NLC-300, we expect 240—120 $\phi^0 Z$ events per fb^{-1} for $m_W < m_{\phi^0} < 2m_W$. The corresponding event numbers for NLC-500 are 60—50 per fb^{-1}. These, of course, are raw event numbers prior to cuts. In the intermediate Higgs mass regime, the dominant Higgs decay mode is $\phi^0 \to b\bar{b}$ (since by assumption, $m_{\phi^0} < 2m_W$). The final state Z boson can be detected in nearly all of its decay modes: $\ell^+\ell^-$, $\nu\bar{\nu}$ (via missing energy) and $q\bar{q}$ (by two jet reconstruction). The obvious backgrounds include $e^+e^- \to 4$ jets and $e^+e^- \to Z + 2$ jets. Suitable cuts can be applied to produce a viable Higgs signal with an integrated luminosity of 10 fb^{-1}. For $m_{\phi^0} \simeq m_Z$, special considerations must be given in order to contend with the irreducible background from $e^+e^- \to ZZ$. At NLC-300 with 10 fb^{-1} the signal rates are high enough for a viable signal-to-background ratio with optimal geometrical cuts. At NLC-500 with the same integrated luminosity, one must resort to some b-tagging in order to enhance the Higgs signal.

As $\sqrt{s}$ increases, a new mechanism for Higgs boson production begins to dominate: $e^+e^- \to \nu\bar{\nu}H^0$ via W^+W^- fusion [fig. 2(c)]. The rate of the W^+W^- fusion

* At present, there is no known technique for observing the Higgs boson via its $t\bar{t}$ decay mode at a hadron supercollider above the large QCD backgrounds.

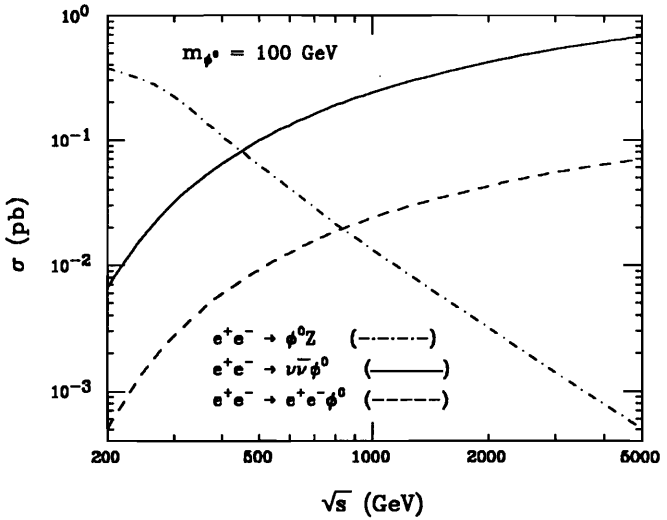

Fig. 3. Total cross sections for Standard Model Higgs production via (i) s-channel Z exchange, (ii) WW-fusion, and (iii) ZZ-fusion as a function of the e^+e^- center-of-mass energy $\sqrt{s}$, for m_{ϕ^0} = 100 GeV. Vector boson fusion cross-sections are taken from ref. 37.

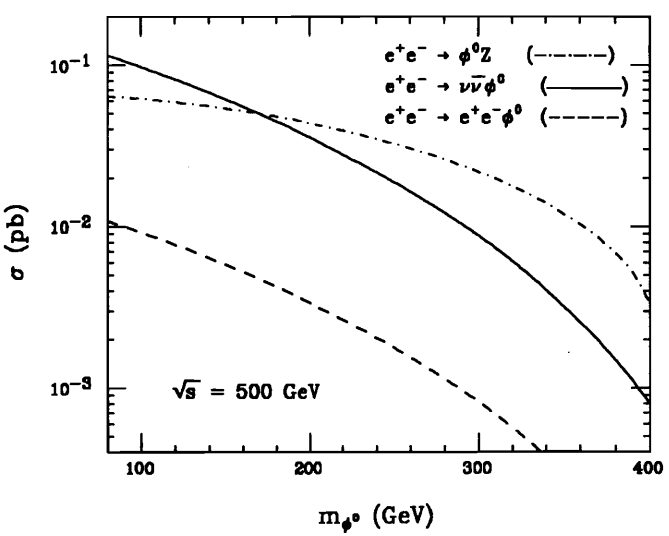

Fig. 4. Total cross sections for Standard Model Higgs production as a function of Higgs mass for $\sqrt{s}$ = 500 GeV. See previous figure caption.

process grows (logarithmically) with energy for fixed Higgs boson mass, in contrast with the annihilation process $e^+e^- \to \phi^0 Z$ which decreases as $1/s$. Thus the relative importance of the W^+W^- fusion process grows as the ratio $s/m^2_{\phi^0}$ increases. These features are illustrated in figs. 3 and 4, where the cross-sections for the W^+W^- (and the related ZZ) fusion processes are shown.[37,39,40] For Higgs masses below $2m_W$, the main background to the WW fusion process arises from $e^+e^- \to e^+e^-b\bar{b}$ (via $\gamma\gamma$ fusion), where the final state e^+e^- is emitted in the very forward direction thereby escaping detection. However, the significance of this background can be substantially reduced by making a cut on $|\cos\theta|$ of the outgoing $b\bar{b}$ pair. The dominant part of the $\gamma\gamma$ fusion background in which the $b\bar{b}$ is emitted near the beam direction can then be eliminated. At NLC-500, Higgs events produced by W^+W^- fusion can be used in addition to $e^+e^- \to \phi^0 Z$ to enhance the overall Higgs signal. In addition, using the W^+W^- fusion mechanism allows one to search for a Higgs boson with $m_{\phi^0} \simeq m_Z$. In this case, the background process is $e^+e^- \to Z\nu\bar{\nu}$. Appropriate cuts at NLC-500 with 10 fb^{-1} leads to a signal-to-background ratio of about 2.[41] Higgs bosons with mass above the intermediate Higgs mass regime will decay dominantly into W^+W^-, ZZ and $t\bar{t}$, as shown in fig. 5. In principle, all three decay modes can be studied at an e^+e^- supercollider. The Higgs mass reach of the NLC, TLC and CLIC is summarized schematically in fig. 6, taken from ref. 9. Based on the initial studies (referred to above and summarized in ref. 9), it is believed that the Higgs mass reach of these colliders are at least equal to $\frac{1}{2}\sqrt{s}$, assuming a minimum integrated luminosity of about $10[\sqrt{s}/1\text{ TeV}]$ fb^{-1}. With further analysis and close attention paid to background rejection, the Higgs mass reach can probably be extended. For example, a recent paper by Barger *et al.*[39] asserts that Higgs bosons up to 350 GeV in mass can be detected at the NLC-500.

Production mechanism that are less important include $e^+e^- \to t\bar{t}\phi^0$ [fig. 2(e) and (f)] and $e^+e^- \to e^+e^-\phi^0$ via $\gamma\gamma$ fusion. The $t\bar{t}\phi^0$ production cross-sections are considerably smaller than that of $\phi^0 Z$, but could provide a measurement of the $\phi^0 t\bar{t}$ coupling, depending on the Higgs and top quark masses and the NLC luminosity.[42] The $\gamma\gamma$ fusion production cross-section[43,44] is smaller than the W^+W^- and ZZ fusion rates due to the fact that the $\gamma\gamma\phi^0$ coupling does not occur at tree-level but is induced at one-loop. Note that the $\gamma\gamma$ fusion process occurs via photons which originate from the e^+e^- beams via the Weizsäcker-Williams process.

A more effective $\gamma\gamma$ luminosity can be obtained by running the NLC in a $\gamma\gamma$ collider mode. By Compton backscattering of laser photons off the NLC electron and positron beams, one can produce high luminosity $\gamma\gamma$ collisions with only a small degradation in the center-of-mass energy.[35,36] In this $\gamma\gamma$ collider mode, the process:

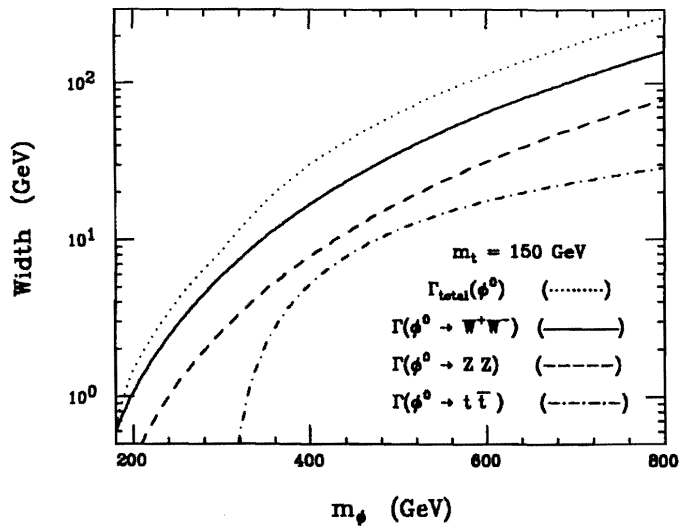

Fig. 5. Total and partial widths for a heavy Standard Model Higgs boson as a function of the Higgs mass, for $m_t = 150$ GeV. Only tree-level widths are shown.

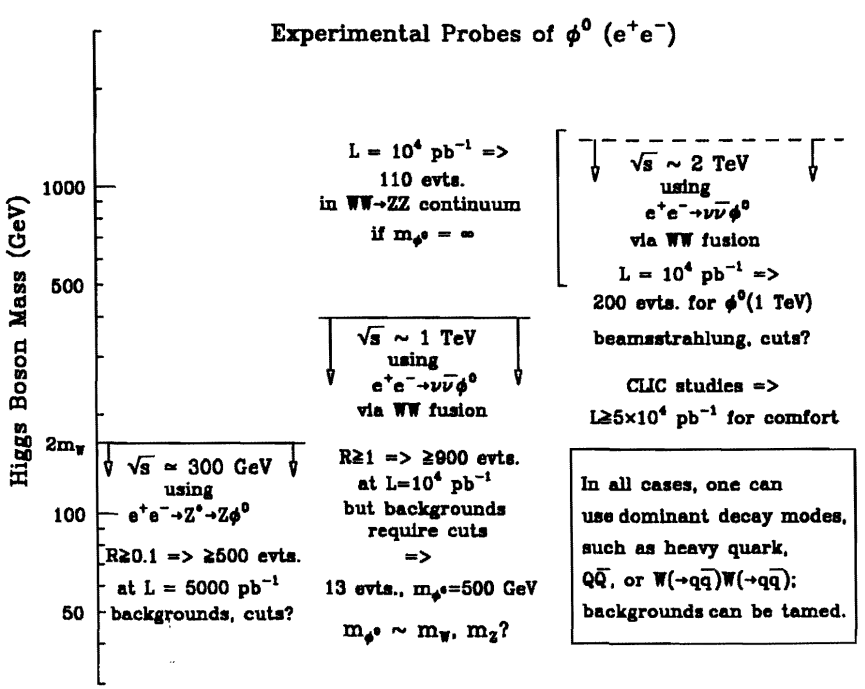

Fig. 6. Experimental reach in m_{ϕ^0} and probable detection modes at future e^+e^- colliders of various energies and luminosities. Taken from ref. 9.

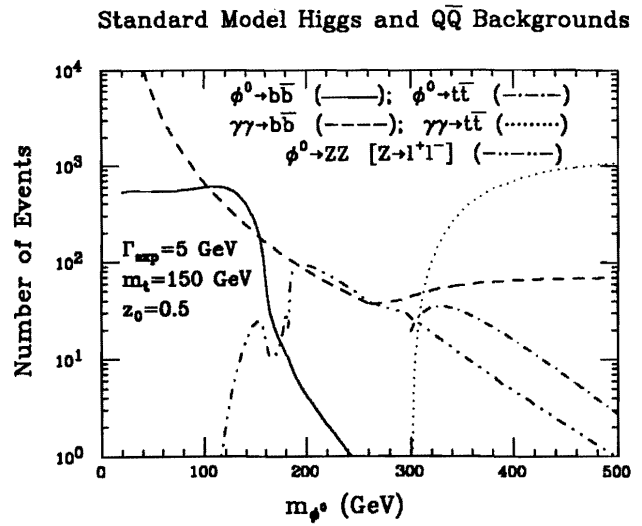

Fig. 7. The number of Standard Model Higgs events per year (based on an integrated luminosity of 20 fb^{-1}) produced via $\phi^0 \to b\bar{b}$, $\phi^0 \to t\bar{t}$, and $\phi^0 \to ZZ$ (where one of the Z's decays either to e^+e^- or $\mu^+\mu^-$) and the corresponding backgrounds [$\gamma\gamma \to b\bar{b}$ and $\gamma\gamma \to t\bar{t}$]. A cut $|\cos\theta| \leq z_0 = 1/2$ has been imposed in the evaluation of the total cross sections for the $Q\bar{Q}$ ($Q = b, t$) final states. The final state experimental resolution is assumed to be $\Gamma_{exp} = 5$ GeV (see ref. 45).

$$\gamma\gamma \to \phi^0 \to \begin{cases} b\bar{b}, & m_{\phi^0} < 2m_W \\ ZZ, & m_{\phi^0} > 2m_Z \end{cases} \tag{2}$$

can provide a viable signature for Higgs boson detection. Assuming that the Higgs boson mass is already known from other experiments, let us operate the $\gamma\gamma$ collider at $\sqrt{s} \simeq m_{\phi^0}$, In fig. 7, the number of Higgs events and background events per year is plotted, based on an integrated luminosity of 20 fb^{-1}. An angular cut has been introduced to suppress the large $\gamma\gamma \to b\bar{b}$ background. Further details of the analysis can be found in ref. 45. The cleanest signature is clearly $\gamma\gamma \to \phi^0 \to ZZ$. This signal is virtually background-free since the process $\gamma\gamma \to ZZ$ is absent at tree-level. (We have not yet examined $\gamma\gamma \to \phi^0 \to W^+W^-$, which must compete with the continuum tree-level process $\gamma\gamma \to W^+W^-$.)

For Higgs bosons with mass below $2m_W$, one must endeavor to separate $\phi^0 \to b\bar{b}$ from the continuum $\gamma\gamma \to b\bar{b}$ events. The angular distribution of background b-quarks in the process $\gamma\gamma \to b\bar{b}$ is given by:

$$\frac{d\sigma}{d\cos\theta} = \frac{4\pi\alpha^2 N_c e_b^4 \beta}{s(1-\beta^2\cos^2\theta)^2}\Big\{1-\beta^4 + (\delta_{\lambda_1\lambda_2}-1)(1+\beta^2\cos^2\theta)[1-\beta^2(2-\cos^2\theta)]\Big\}, \tag{3}$$

where $\beta^2 \equiv 1 - 4m_b^2/s$, $e_b = -1/3$, $N_c = 3$, and λ_1 and λ_2 are the initial state photon helicities. The angular distribution of b-quarks from $\gamma\gamma \to \phi^0 \to b\bar{b}$ is isotropic and the cross-section vanishes for $\lambda_1 \neq \lambda_2$. Consider first the case of unpolarized beams. Since β is very close to 1, we see that an angular cut is useful in reducing background since most of the background b-quarks are produced near the beam direction. According to the results of fig. 7, Higgs bosons over a limited mass range can be detected in their $b\bar{b}$ decay mode above background. If the initial beams are polarized, one may be able to reduce this background further.[36,46] By choosing $\lambda_1 = \lambda_2$, one can significantly suppress the background without affecting the signal rate. Even partially polarized beams would increase the signal-to-background ratio.* Finally, note that the Higgs decay into $t\bar{t}$ pairs is overwhelmed by $\gamma\gamma \to t\bar{t}$, where the angular cuts are not very effective.

One can also consider various production processes in which multiple Higgs bosons[47] or Higgs bosons in association with vector bosons[48] are produced. The cross sections tend to be very small, and only for Higgs masses lighter than about 50 GeV could such processes be measured at e^+e^- supercolliders considered in this report.

In all the analyses presented above, the tree-level couplings of the Standard Model were employed in making predictions for Higgs production and decay rates. Once the Higgs boson is discovered, it may be possible to perform a number of precision measurements of Higgs processes which would be sensitive to the one-loop electroweak radiative corrections. Although these are clearly second generation experiments, it does illustrate a class of measurements which could only be performed at a future e^+e^- supercollider. The typical size of such one-loop effects is illustrated in fig. 8 which was presented by B. Kniehl in the parallel sessions. The one-loop corrections to the rates for Higgs decay into ZZ and W^+W^- tend to be quite small for $m_{\phi^0} \lesssim 500$ GeV.[49,50] However, if the virtual effects of physics beyond the Standard Model are included, such as a heavy fourth generation of quarks, it is possible to enhance the effects of the one-loop corrections[49–52] as illustrated

* A note of caution must be raised at this point. If one of the b quarks radiates a gluon, the resulting background process is no longer suppressed when $\lambda_1 = \lambda_2$. One can experimentally reject events with hard gluon emission; however the implications of soft gluon emission have yet to be determined. I thank V.A. Khoze for raising this issue.

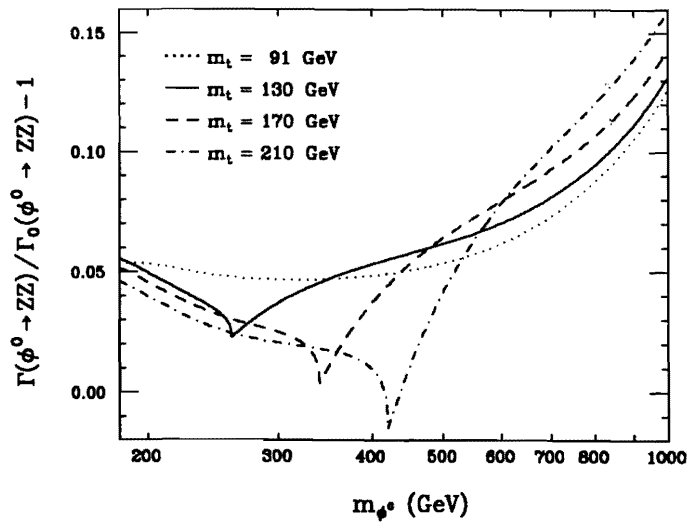

Fig. 8. Standard Model radiative corrections for $\Gamma(\phi^0 \to ZZ)$ in the modified on-mass-shell scheme of ref. 53 for selected values of m_t. Γ_0 is the tree-level width and Γ includes the one-loop radiative corrections. Taken from ref. 49.

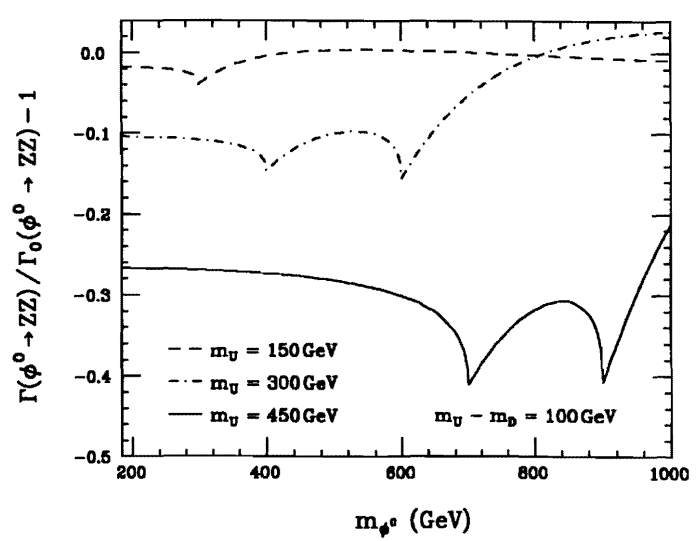

Fig. 9. Contributions of a heavy quark doublet, (U, D), to $\Gamma(\phi^0 \to ZZ)$ for selected values of m_U assuming a fixed mass splitting of $m_U - m_D = 100$ GeV. See caption to fig. 8. Taken from ref. 49.

in fig. 9.[49] Radiative corrections to the Higgs production process $e^+e^- \to \phi^0 Z$ have also been computed.[54,55] These corrections also tend to be quite small and depend sensitively on the value of the Higgs mass and the center-of-mass energy.

3. Phenomenology of Nonminimal Higgs Sectors

As discussed in section 1, the Standard Model with minimal Higgs content is not expected to be the ultimate theoretical structure responsible for electroweak symmetry breaking. In theories beyond the minimal model, one must decide whether the Higgs mechanism involves weakly coupled or strongly coupled physics. Theories of electroweak symmetry breaking involving weakly coupled Higgs sectors are straightforward to analyze since perturbative techniques can be used to reliably compute the details of the Higgs phenomenology. In contrast, strongly interacting theories of electroweak symmetry breaking are theoretically very challenging. So far, no "standard" model of this type has been formulated whose predictions are definite enough to serve as a benchmark for comparison with experimental data. In this report, I will only consider theories of electroweak symmetry breaking with weakly coupled extended Higgs sectors. Among such theories, those incorporating "low-energy" supersymmetry are particularly attractive in that they have the potential to provide an understanding of the origin of the electroweak scale and the large hierarchy between this scale and the Planck scale. Such models will be discussed further in section 4.

Since very little is known about the properties of the Higgs sector, it may seem that there are few constraints on its extension. However, given that the ρ parameter of electroweak physics is equal to 1 with about a 1% experimental uncertainty,[3,56] the most natural choice for an extended Higgs sector consists of a model with multiple copies of $Y = \pm 1$, weak doublet Higgs multiplets (and perhaps Higgs singlets as well). For example, the (tree-level) Higgs sector of the minimal supersymmetric model (MSSM) is a CP-conserving two-Higgs-doublet model, with restricted Higgs-fermion couplings in which the $Y = -1$ [$Y = +1$] Higgs doublet couples only to down-type [up-type] fermions.

In order to describe the variety of new phenomenology in models with extended Higgs sectors, it is instructive to study the simplest extended Higgs sector consisting of precisely two weak Higgs doublets.[57] For simplicity, I will assume that the Higgs sector is CP-conserving (although this is automatic in the MSSM as mentioned above). The physical Higgs bosons of this model consist of a charged Higgs boson pair ($H^\pm$), a CP-odd neutral scalar (A^0) and two CP-even neutral scalars (h^0 and H^0, where the notation indicates the relative masses: $m_{h^0} \leq m_{H^0}$). In determining the CP-even Higgs mass eigenstates, one must diagonalize a 2×2

squared-mass matrix. The angle of diagonalization is denoted by α and appears in the Feynman rules of the CP-even Higgs boson interactions. In addition, an important parameter of the model is:

$$\tan\beta = \frac{v_2}{v_1}, \tag{4}$$

where v_1 and v_2 are the vacuum expectation values of the real part of the neutral components of the two Higgs doublet fields, respectively.* (The quantity $v_1^2 + v_2^2 = 2m_W^2/g^2$ is fixed by the W mass.)

The phenomenology of the two-Higgs doublet model depends in detail on the various couplings of the Higgs bosons to gauge bosons, Higgs bosons and fermions. The Higgs couplings to gauge bosons follow from gauge invariance and are thus model independent. For example, using the symbol ϕ^0 for the minimal Higgs boson of the Standard Model, the coupling of the two CP-even Higgs bosons to W and Z pairs is given in terms of the angles α and β by:

$$\begin{aligned} g_{h^0VV} &= g_{\phi^0VV}\sin(\beta-\alpha) \\ g_{H^0VV} &= g_{\phi^0VV}\cos(\beta-\alpha), \end{aligned} \tag{5}$$

where $g_{\phi^0VV} \equiv g_V m_V$ and

$$g_V = \begin{cases} g, & V = W, \\ g/\cos\theta_W, & V = Z. \end{cases} \tag{6}$$

There are no tree-level couplings of A^0 or $H^\pm$ to VV. Gauge invariance also determines the strength of the trilinear couplings of one gauge boson to two Higgs bosons. For example,

$$\begin{aligned} g_{h^0A^0Z} &= \frac{g\cos(\beta-\alpha)}{2\cos\theta_W}, \\ g_{H^0A^0Z} &= \frac{-g\sin(\beta-\alpha)}{2\cos\theta_W}, \end{aligned} \tag{7}$$

In the examples shown above, some of the couplings can be suppressed if either $\sin(\beta-\alpha)$ or $\cos(\beta-\alpha)$ is very small. Indeed this does occur in various models. If the theory yields a Higgs mass spectrum in which the h^0 is considerably lighter than the other physical Higgs scalars, then the h^0 couplings will typically approach their

* In the MSSM, v_1 [v_2] is the vacuum expectation value of the Higgs field that couples to down-type [up-type] fermions.

Standard Model values.[58] In this limit, $\cos(\beta-\alpha)\to 0$. Clearly, all the couplings cannot vanish simultaneously; from the expressions above, we see that the following sum rules must hold:

$$g^2_{H^0VV}+g^2_{h^0VV}=g^2_{\phi^0VV}\,,$$
$$g^2_{h^0A^0Z}+g^2_{H^0A^0Z}=\frac{g^2}{4\cos^2\theta_W}\,, \tag{8}$$

which hold separately for $V=W$ or Z. These results are a consequence of the tree-unitarity of the electroweak theory.[59] Moreover, if we focus on a given CP-even Higgs state, we note that its couplings to VV and A^0V cannot be simultaneously suppressed, since eq. (5)–(7) implies that:

$$g^2_{hZZ}+4m^2_Z g^2_{hA^0Z}=\frac{g^2m^2_Z}{\cos^2\theta_W}\,, \tag{9}$$

for $h=H^0$ or h^0.

The Higgs couplings to fermions are model dependent, although their form can be constrained by discrete symmetries that are often imposed in order to avoid tree-level flavor changing neutral currents mediated by Higgs exchange.[60] An example of a model that respects this constraint is one in which one Higgs doublet (before symmetry breaking) couples exclusively to down-type fermions and the other Higgs doublet couples exclusively to up-type fermions. This is the pattern of couplings found in the minimal supersymmetric model (MSSM). The results in this case are easily summarized. The couplings of the neutral Higgs bosons relative to the canonical Standard Model values are given by (using 3rd family notation):

$$\begin{array}{llll} H^0t\bar{t}: & \dfrac{\sin\alpha}{\sin\beta} & H^0b\bar{b}: & \dfrac{\cos\alpha}{\cos\beta} \\[2ex] h^0t\bar{t}: & \dfrac{\cos\alpha}{\sin\beta} & h^0b\bar{b}: & \dfrac{-\sin\alpha}{\cos\beta} \\[2ex] A^0t\bar{t}: & \gamma_5\cot\beta & A^0b\bar{b}: & \gamma_5\tan\beta, \end{array} \tag{10}$$

(the γ_5 indicates a pseudoscalar coupling), and the charged Higgs boson coupling is given by:

$$g_{H^-t\bar{b}}=\frac{g}{2\sqrt{2}m_W}\,[m_t\cot\beta(1+\gamma_5)+m_b\tan\beta(1-\gamma_5)]. \tag{11}$$

Finally, the 3-point and 4-point Higgs self-couplings depend on the details of the two-Higgs-doublet potential. In the MSSM, these couplings are related to gauge couplings and therefore take on rather simple forms. A comprehensive set of Feynman rules for the Higgs sector of the MSSM can be found in ref. 9.

Let us first consider the phenomenology of the neutral CP-even Higgs bosons. The production mechanisms are identical to those of the minimal Higgs boson discussed in section 2. If we examine the diagrams of fig. 2, we see that nearly all the Higgs production processes depend on the Higgs coupling to heavy vector boson pairs (VV). Note that the couplings to VV are suppressed compared to the ϕ^0VV coupling of the Standard Model [see eq. (5)]. The square of the appropriate suppression factors must then be applied to the cross-section results obtained in section 2. Modified Higgs-fermion couplings affect two Higgs production mechanisms: $e^+e^-\to t\bar{t}h$ and $\gamma\gamma\to h$ (where $h=h^0,\,H^0$). In addition, the neutral Higgs decay relative branching ratios into fermion pairs can deviate significantly from those of the Standard Model when $\tan\beta$ differs substantially from 1. For example, for $\tan\beta\gg 1$ the Higgs coupling to $b\bar{b}$ pairs is greatly enhanced [see eq. (10)], and this channel can even be competitive with $t\bar{t}$ when the latter is kinematically allowed.

The Higgs phenomenology just described is a simple extension of that of the minimal Standard Model, differing only by some enhanced and some suppressed couplings. However, the extended Higgs sector introduces genuinely new Higgs phenomena. The two most important new processes are shown in fig. 10.

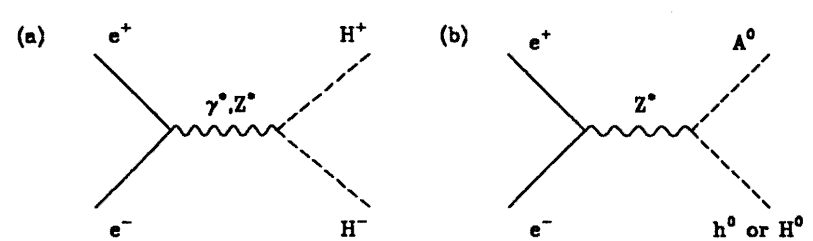

Fig. 10. The primary production mechanisms for charged Higgs pairs and the CP-odd neutral Higgs boson (A^0) in e^+e^- collisions.

Charged Higgs boson pairs can be produced via s-channel γ and Z exchange. It is convenient to present cross-sections in units of R, where one unit of R is equal to: $\sigma_{\rm pt}\equiv\sigma(e^+e^-\to\gamma^*\to\mu^+\mu^-)=4\pi\alpha^2/3s=86.8$ fb/[s (TeV^2)]. The asymptotic result for $\sigma(e^+e^-\to H^+H^-)$ in units of R (for $s\gg m^2_Z, 4m^2_{H^\pm}$) is given by:[61]

$$\frac{\sigma_{\rm asympt}}{\sigma_{\rm pt}}=\frac{1+4\sin^4\theta_W}{8\sin^4 2\theta_W}\simeq 0.308\,. \tag{12}$$

(This should be compared with 0.25 units of R if Z-exchange is not included.) Charged Higgs masses up to about $0.4\sqrt{s}$ will be detectable at an e^+e^- collider

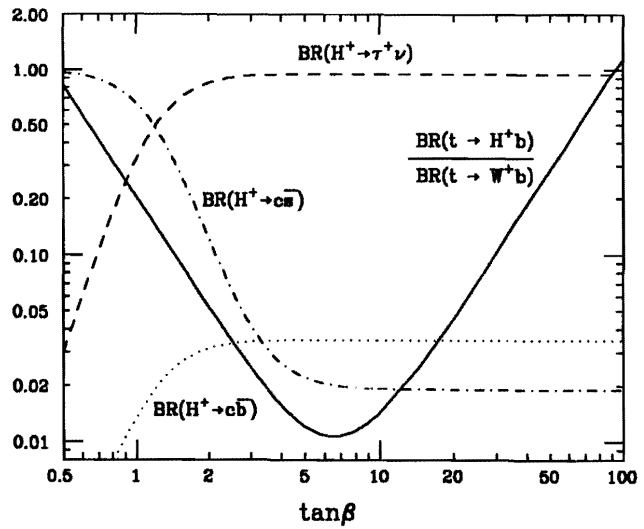

Fig. 11. Various branching fractions involving the charged Higgs boson as a function of $\tan\beta$, assuming $m_{H^\pm} = 150$ GeV and $m_t = 200$ GeV. In this case, nearly all top quarks decay into either W^+b or H^+b final states. (The H^+ branching ratios are only sensitive to the fact that $m_{H^\pm} \leq m_t + m_b$.) The above results assume a Higgs-fermion coupling in which only the first [second] Higgs doublet couples exclusively to down-type [up-type] fermions. Other parameters are: $m_b = 4.7$ GeV, $m_c = 1.5$ GeV, $m_\tau = 1.784$ GeV, and the CKM mixing elements $V_{cs} = 0.974$ and $V_{cb} = 0.044$. It is further assumed that the decays $H^\pm \to W^\pm h^0$ and $H^\pm \to W^\pm A^0$ are kinematically forbidden.

with an integrated luminosity of 10^3 inverse units of R.[62] Mechanisms for single $H^\pm$ production also exist. If $m_t > m_{H^\pm} + m_b$, then $e^+e^- \to t\bar{t}$ followed by $t \to bH^+$ will provide a competitive source of charged Higgs bosons, depending on the relative importance of the latter decay mode compared to $t \to bW^+$ as shown in fig. 11.[61,63] If $t \to bH^+$ is not kinematically allowed, single Higgs production via $e^+e^- \to t\bar{b}H^+$ can occur only via radiation off a virtual b or t quark, and leads to a production cross-section substantially less than 0.1 units of R. The charged Higgs boson can be detected in its leptonic ($\tau\nu$) or two-jet decay modes. The relative branching ratios depend on $\tan\beta$ as shown in fig. 11. If kinematically allowed, the decay modes $H^\pm \to W^\pm h^0$ and/or $H^\pm \to W^\pm A^0$ can also be significant.

In contrast to the production of the CP-even neutral Higgs bosons described above, it is more difficult to produce the CP-odd A^0 since there is no tree-level A^0VV coupling. The A^0 production mode that is available is $Z^* \to A^0h^0$ or A^0H^0. The cross sections for this process is easily computed, and the result is:[44]

$$\sigma(e^+e^- \to A^0h^0) = \left(\frac{8\sin^4\theta_W - 4\sin^2\theta_W + 1}{\cos^4\theta_W}\right) \frac{g^4\cos^2(\beta-\alpha)\kappa^3}{192\pi\sqrt{s}\left[(s-m_Z^2)^2 + \Gamma_Z^2 m_Z^2\right]}, \tag{13}$$

where κ is the center-of-mass momentum of one of the final state Higgs bosons. For $\sigma(e^+e^- \to A^0H^0)$, replace $\cos(\beta-\alpha)$ with $\sin(\beta-\alpha)$ in eq. (13). The detection of this process is possible [64] if $m_{A^0}+m_{h^0}$ (or $m_{A^0}+m_{H^0}$) is not too large compared to the machine energy. For instance, if the ZA^0H^0 is maximal [*i.e.*, $\cos^2(\beta-\alpha) = 1$], then the cross section for $e^+e^- \to Z^* \to A^0 + H^0$ can be as large as 0.1 units of R.[44] Mechanisms which produce the A^0 singly such as $e^+e^- \to t\bar{t}A^0$ and $e^+e^- \to e^+e^-A^0$ (via $\gamma\gamma$ fusion through a top-quark loop) have cross-sections that are substantially less than 0.1 units of R. In the case of $\gamma\gamma$ fusion, the small cross-section is due in part to the softness of the Weiszäcker-Williams spectrum. In the $\gamma\gamma$ collider mode discussed at the end of section 2, the production rate for A^0 is large enough to be studied over some of the range of parameter space. Specific calculations in the context of the MSSM will be discussed at the end of section 4.

Once the Higgs bosons are produced, they are detected by their final state decay products. In the Standard Model, the Higgs boson decays almost entirely into W^+W^- and ZZ for Higgs masses above $2m_Z$, and into $b\bar{b}$ for Higgs masses in the intermediate mass region. For Higgs bosons of the two-doublet model, the decay branching ratios pattern is more complex. The CP-even neutral Higgs decays resemble those of the minimal Higgs boson, unless the corresponding hVV coupling is greatly suppressed. For example, in the MSSM, $\cos(\beta-\alpha)$ is very small over nearly all of the parameter space.[12] As a result, the decay rate for $H^0 \to VV$ is greatly suppressed, and typically, the heaviest fermion pair that is kinematically allowed provides the largest branching fraction. The absence of tree-level decays of A^0 and $H^\pm$ into VV channels also has a similar effect. However, new decay channels are also available which could have substantial branching fractions: $H^0 \to ZA^0$, h^0h^0, A^0A^0, H^+H^-; $A^0 \to Zh^0$ and $H^\pm \to W^\pm h^0$, $W^\pm A^0$. The decays into vector boson Higgs boson final states can be quite significant (due to the possibility of a longitudinal gauge boson in the final state) unless suppressed by an "angle factor" [*e.g.*, see eq. (7)]. The decay widths for modes with two Higgs boson final states depends on model-dependent details of the Higgs self-couplings. Specific examples of Higgs decay branching ratios in the MSSM will be exhibited at the end of section 4. In the MSSM, other possibilities arise if Higgs decay into supersymmetric final states is kinematically allowed.[65] In this case, the supersymmetric decay modes can dominate (decays into charginos/neutralino pairs will be the most important), in which case the methods for Higgs detection must be radically altered. In such a scenario, it is likely that the supersymmetric particle spectrum will have to be discovered and elucidated before the heavier Higgs bosons of the theory with significant supersymmetric decay modes can be unambiguously identified.

The exploration of the nonminimal Higgs sector at a future collider requires the identification of scalar states and the determination of their various properties, including electroweak quantum numbers and coupling strengths. For example, to distinguish h^0 from A^0, it is sufficient to identify a ZA^0h^0 vertex, since the Z does not couple to two scalars with the same CP quantum number. (In principle, one could also try to distinguish a scalar and pseudoscalar coupling of the Higgs boson to fermion pairs, although this requires a substantial amount of data.[66]) The e^+e^- supercolliders are ideally suited for this task. Background cross-sections (with suitably applied cuts) tend to be of order 1 unit of R or less, which allows for a favorable signal-to-noise ratio in the search for new physics. In particular, W and Z bosons can be effectively isolated in their hadronic decay modes. As a result, Higgs decays involving gauge bosons in the final state can be studied in detail without the necessity of applying severe cuts (*e.g.*, the requirement of leptonic vector boson decay). In comparison, the effectiveness of the SSC and LHC for nonminimal Higgs hunting is limited. In the case of the charged Higgs boson, a hadron supercollider can probably discover the $H^\pm$ if it is produced in top-quark decays[32,67–70] (as discussed above). If $t\bar{b}$ is the dominant decay of the H^+, there is no known technique at present to discover the $H^\pm$ at the SSC and LHC.[67] In the case of A^0, if $A^0 \to t\bar{t}$ is kinematically allowed and the dominant decay mode, then it will be very difficult to discover at a hadron supercollider.* Other cases present a difficult but perhaps surmountable challenge.[71–75] For the CP-even neutral Higgs bosons, the techniques developed for the minimal Higgs of the Standard Model apply.[32,72–76] For masses in the intermediate mass regime, both CP-even and CP-odd Higgs bosons can probably be detected. However, the proposed analyses rely on very severe cuts in order to reduce backgrounds. The end result often leaves a data sample with a few tens of events or less. Even if the case could be made that the signal corresponds to a Higgs boson, details of the corresponding Higgs properties will remain scarce. For heavy CP-even Higgs bosons, the case where the H^0VV coupling is suppressed poses a serious problem for the Higgs search. To reiterate, it is very difficult to discover a Higgs boson whose dominant decay mode is into $t\bar{t}$.* Thus, a hadron supercollider is primarily a discovery machine in the case of a nonminimal Higgs sector. The cross-sections for nonminimal Higgs production are not suppressed at the SSC and LHC, and one typically expects anywhere from 10^5 to 10^7 Higgs bosons produced per SSC year (depending on the choice of parameters). However, the isolation of these Higgs events above background presents a serious challenge. In certain ranges of parameter space, some of the nonminimal Higgs bosons will simply be lost in the large QCD backgrounds. In contrast, the size of the Higgs cross section is the primary factor that determines the viability of the Higgs search at future e^+e^- supercolliders. Assuming that the Higgs cross-sections are sufficiently large, a detailed investigation of the nonminimal Higgs spectrum is viable.

* In this case the only detectable signal may be $pp \to t\bar{t}h$ ($h = A^0$ or H^0) where $h \to t\bar{t}$. This assumes that $t\bar{t}t\bar{t}$ events, in which the invariant mass of one of the $t\bar{t}$ pairs is equal to m_h, can be successfully isolated from the QCD background.

4. The Higgs Sector of the Minimal Supersymmetric Model

In section 3, the two-doublet Higgs model was put forward as the canonical example of a nonminimal Higgs sector. This model depends on (at least) six free parameters: four physical Higgs masses, the CP-even Higgs mixing angle α and the ratio of vacuum expectation values, $\tan\beta$. In addition, there is some freedom in the choice of the Higgs potential and the Higgs-fermion interaction. As a result of this very large parameter space, the Higgs phenomenology of the most general two-Higgs-doublet model is difficult to pin down. The size of Higgs cross-sections and the pattern of Higgs decays depend on a large number of unknown parameters. The observability of Higgs bosons at future colliders can in some cases depend critically on these free parameters.

The minimal supersymmetric model (MSSM) is very appealing for a number of reasons outlined in section 1. In the context of Higgs physics, the MSSM provides the simplest and most predictive extended Higgs sector.[77] In particular, the tree-level Higgs-fermion interaction and the Higgs potential are uniquely specified. As a result, the six free parameters listed above collapse to two. For convenience, I shall choose these parameters to be $\tan\beta$ and m_{A^0}; in terms of these the other parameters become derived quantities whose values are predicted. For example, in the MSSM, the quartic couplings of the Higgs potential can be expressed in terms of the gauge couplings. This is a result of the supersymmetry and is not affected (at tree-level) by supersymmetry breaking. From the Higgs potential, the neutral CP-even Higgs squared-mass matrix can be obtained:

$$\mathcal{M}^2 = \begin{pmatrix} m_{A^0}^2 \sin^2\beta + m_Z^2\cos^2\beta & -(m_{A^0}^2 + m_Z^2)\sin\beta\cos\beta \\ -(m_{A^0}^2 + m_Z^2)\sin\beta\cos\beta & m_{A^0}^2\cos^2\beta + m_Z^2\sin^2\beta \end{pmatrix} . \tag{14}$$

We can easily evaluate the eigenvalues of $\mathcal{M}^2$. These are the squared masses of the two CP-even Higgs scalars

$$m_{H^0,h^0}^2 = \tfrac{1}{2}\left[m_{A^0}^2 + m_Z^2 \pm \sqrt{(m_{A^0}^2 + m_Z^2)^2 - 4m_Z^2 m_{A^0}^2\cos^2 2\beta}\right] . \tag{15}$$

Following the conventions of ref. 11, the diagonalizing angle is α, with

$$\cos 2\alpha = -\cos 2\beta \left(\frac{m_{A^0}^2 - m_Z^2}{m_{H^0}^2 - m_{h^0}^2} \right), \qquad \sin 2\alpha = -\sin 2\beta \left(\frac{m_{H^0}^2 + m_{h^0}^2}{m_{H^0}^2 - m_{h^0}^2} \right). \quad (16)$$

Finally, the following inequalities are easily established:

$$\begin{aligned} & m_{h^0} \leq m_{A^0} \\ & m_{h^0} \leq m|\cos 2\beta| \leq m_Z, \qquad \text{with } m \equiv min(m_Z, m_{A^0}) \\ & m_{H^0} \geq m_Z. \end{aligned} \quad (17)$$

By a separate computation, the charged Higgs mass is also determined:

$$m_{H^\pm}^2 = m_{A^0}^2 + m_W^2. \quad (18)$$

All the above results are tree-level predictions of the MSSM. For example, the bound $m_{h^0} \leq m_Z$, if reliable, would have significant implications for future experiments at LEP-II. In principle, experiments running at LEP-II operating at design luminosity would either discover the Higgs boson or rule out the MSSM. (Whether this is possible to do in practice depends on whether these experiments can rule out a Higgs boson with $m_{h^0} \approx m_Z$.) However, $m_{h^0} \leq m_Z$ need not be respected when radiative corrections are incorporated. In general, one might expect the size of the (electroweak) radiative corrections to the Higgs squared masses to be of order $g^2 m_Z^2/4\pi$, which would shift the Higgs masses by (at most) a few GeV. However, we encounter a surprise when we consider the effects of radiative corrections on the tree-level results presented above.[78–81] In the radiative corrections to the neutral CP-even Higgs squared-mass matrix, the 22-element is shifted by a term proportional to $(g^2 m_t^4/m_W^2)\ \ln(M_{\tilde{t}}^2/m_t^2)$. Such a term arises from an incomplete cancellation between top-quark and top-squark loop contributions to the neutral Higgs boson self-energy. If m_t is large, this term significantly alters the tree-level predictions given above.

Hempfling and I computed the exact one-loop expression for the light Higgs mass bound, as a function of all the relevant supersymmetric parameters.[79] This bound is saturated in the formal limit where $\tan\beta \to \infty$ (with all down-type fermions masses equal to zero) and $m_{A^0} \geq m_Z$, m_{h^0}. The expression we obtained is quite cumbersome, though is straightforward to evaluate numerically. However, it is useful to display an approximate expression, valid for a certain range of supersymmetric parameters. If all supersymmetric mass parameters are roughly of order $M_{\rm SUSY}$ and $m_Z < m_t \ll M_{\rm SUSY}$, then

$$\begin{aligned} m_{h^0}^2 - m_Z^2 \lesssim \frac{3g^2 m_Z^4}{16\pi^2 m_W^2} \Bigg\{ & \ln\left(\frac{M_{\tilde{Q}}^2}{m_t^2}\right) \left[\frac{2m_t^4 - m_t^2 m_Z^2}{m_Z^4} + \tfrac{1}{6}\left(1 - \tfrac{8}{3}s_W^2 + \tfrac{32}{9}s_W^4\right) \right] \\ & + \ln\left(\frac{M_{\tilde{Q}}^2}{m_Z^2}\right) \Bigg[\tfrac{1}{3}\left(1 - \tfrac{8}{3}s_W^2 + \tfrac{32}{9}s_W^4\right) + \tfrac{1}{2}\left(1 - \tfrac{4}{3}s_W^2 + \tfrac{8}{9}s_W^4\right) \\ & + \tfrac{1}{3}\left(1 - 2s_W^2 + 4s_W^4\right) \Bigg] + \frac{m_t^2}{3m_Z^2} \Bigg\} \\ & - \frac{g^2 m_Z^4}{48\pi^2 m_W^2} \left[(27 - 54s_W^2 + 32s_W^4) \ln\left(\frac{M_{\tilde{\chi}}^2}{m_Z^2}\right) - (1 - 2s_W^2 + 2s_W^4) \ln\left(\frac{m_{A^0}^2}{m_Z^2}\right) \right], \end{aligned} \quad (19)$$

where $s_W \equiv \sin\theta_W$, $M_{\tilde{Q}}$ is a common soft-supersymmetry-breaking diagonal squark mass term, and $M_{\tilde{\chi}}$ is a common neutralino/chargino mass. The radiatively corrected light Higgs mass bound will be written as:

$$m_{h^0} \leq m_Z + \Delta m_h, \quad (20)$$

which defines the quantity Δm_h. A numerical calculation of Δm_h is displayed in fig. 12. As advertised, the dominant correction to the tree-level formula increases as the fourth power of m_t, and therefore can be quite large. Nevertheless, for values of $m_t \lesssim 250$ GeV, the perturbative one-loop calculation is reliable. This can be verified by estimating the largest two-loop contributions to Δm_h and showing that the one-loop result is stable.[82]

It is also evident from eq. (19) that the dependence of the squared Higgs mass shift on $M_{\tilde{Q}}^2$ is logarithmic. Thus, even if $M_{\tilde{Q}}$ is significantly smaller than 1 TeV, Δm_h can be appreciable if m_t is sufficiently large. This is illustrated in fig. 13, where Δm_h is plotted as a function of $M_{\tilde{Q}}$ for $m_t = 100$, 150 and 200 GeV. These results are based on an exact numerical one-loop computation; the approximate formula given in eq. (19) is unreliable for values of $M_{\tilde{Q}}$ approaching m_t.

One can also compute radiative corrections to the full CP-even Higgs mass-squared matrix. Various calculations employing various approximations have appeared in the literature.[81,83–88] Here, I will present the results based on a calculation of the mass-squared matrix in which all leading logarithmic one-loop terms are included. Details can be found in ref. 84. The resulting matrix elements for

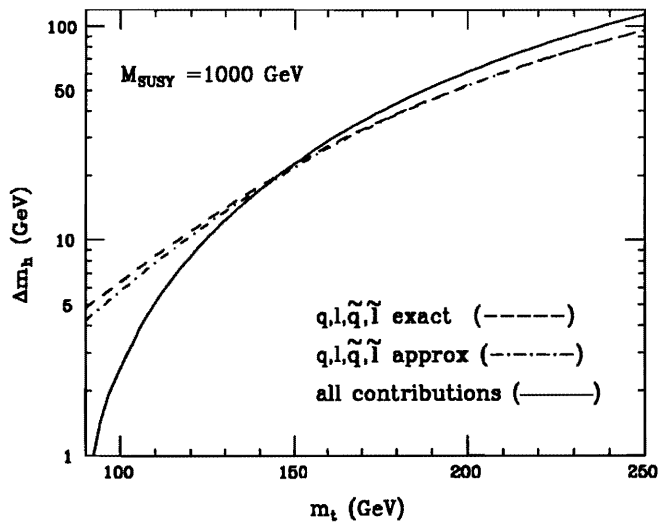

Fig. 12. The light Higgs mass bound ($m_{h^0} \leq m_Z + \Delta m_h$) including one-loop radiative corrections. The dashed line denotes the contribution to Δm_h due to three generations of quarks, leptons, and their supersymmetric scalar partners (assumed to have a common soft-supersymmetry breaking mass of $M_{\tilde{Q}} = 1$ TeV); $\tilde{t}_L$-$\tilde{t}_R$ mixing is neglected. The dot-dashed line is a plot of the corresponding contribution to eq. (19). The solid line includes *all* contributions to the exact one-loop calculation of Δm_h where all supersymmetric mass parameters (including the A parameter that controls top-squark mixing) are equal to $M_{\rm SUSY} = 1$ TeV. Taken from ref. 79.

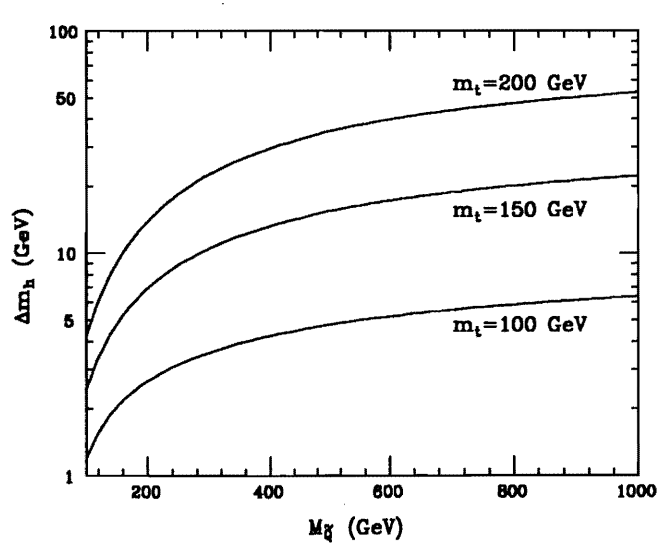

Fig. 13. The contribution to Δm_h of three generations of quarks, leptons, and their supersymmetric scalar partners as a function of the common soft-supersymmetry breaking scalar mass, $M_{\tilde{Q}}$, for three different values of the top quark mass. Squark mixing is neglected.

the mass-squared matrix to one-loop leading logarithmic accuracy are given by:

$$
\begin{aligned}
\mathcal{M}^2_{11} &= m^2_{A^0} s^2_\beta + m^2_Z c^2_\beta + \frac{g^2 m^2_Z c^2_\beta}{96\pi^2 c^2_W}\Bigg[P_t \ln\left(\frac{M^2_{\rm SUSY}}{m^2_t}\right) \\
&\quad + \left(12N_c \frac{m^4_b}{m^4_Z c^4_\beta} - 6N_c \frac{m^2_b}{m^2_Z c^2_\beta} + P_f + P_g + P_{2H}\right) \ln\left(\frac{M^2_{\rm SUSY}}{m^2_Z}\right)\Bigg] \\
\mathcal{M}^2_{22} &= m^2_{A^0} c^2_\beta + m^2_Z s^2_\beta + \frac{g^2 m^2_Z s^2_\beta}{96\pi^2 c^2_W}\Bigg[\left(P_f + P_g + P_{2H}\right) \ln\left(\frac{M^2_{\rm SUSY}}{m^2_Z}\right) \\
&\quad + \left(12N_c \frac{m^4_t}{m^4_Z s^4_\beta} - 6N_c \frac{m^2_t}{m^2_Z s^2_\beta} + P_t\right) \ln\left(\frac{M^2_{\rm SUSY}}{m^2_t}\right)\Bigg] \\
\mathcal{M}^2_{12} &= -s_\beta c_\beta \Bigg\{ m^2_{A^0} + m^2_Z + \frac{g^2 m^2_Z}{96\pi^2 c^2_W}\Bigg[\left(P_t - 3N_c \frac{m^2_t}{m^2_Z s^2_\beta}\right) \ln\left(\frac{M^2_{\rm SUSY}}{m^2_t}\right) \\
&\quad + \left(-3N_c \frac{m^2_b}{m^2_Z c^2_\beta} + P_f + P'_g + P'_{2H}\right) \ln\left(\frac{M^2_{\rm SUSY}}{m^2_Z}\right)\Bigg]\Bigg\},
\end{aligned}
\tag{21}
$$

assuming $m_{A^0} \lesssim \mathcal{O}(m_Z)$, where

$$
\begin{aligned}
P_t &\equiv N_c(1 - 4e_u s^2_W + 8e^2_u s^4_W), \\
P_f &\equiv N_G\{N_c[2 - 4s^2_W + 8(e^2_d + e^2_u)s^4_W] + [2 - 4s^2_W + 8s^4_W]\} - P_t, \\
P_g &\equiv -44 + 106 s^2_W - 62 s^4_W, \\
P'_g &\equiv 10 + 34 s^2_W - 26 s^4_W, \\
P_{2H} &\equiv -10 + 2s^2_W - 2s^4_W, \\
P'_{2H} &\equiv 8 - 22 s^2_W + 10 s^4_W.
\end{aligned}
\tag{22}
$$

In the above formulae, the number of generations $N_G = 3$, the number of colors $N_c = 3$ and the electric charges of the quarks are $e_u = 2/3$, $e_d = -1/3$. The subscripts t, f, g and $2H$ indicate that these are the contributions from the top quark, the fermions (leptons and quarks excluding the top quark) the gauge bosons and the two Higgs doublets, respectively. Diagonalizing the squared mass matrix given by eq. (21) yields the radiatively corrected Higgs mixing angle α. The leading log formulae presented above are expected to be accurate as long as: (i) the scale characterizing supersymmetric masses, $M_{\rm SUSY}$ is large, and sufficiently separated from m_Z (say, $M_{\rm SUSY} \gtrsim 500$ GeV), (ii) m_t is significantly above m_Z (say, $m_t \gtrsim 150$ GeV) while still being small compared to $M_{\rm SUSY}$, and (iii) the squark mixing parameters are not unduly large. I have checked these results by comparing the predictions derived from eq. (21) with those of ref. 83 which includes non-leading logarithmic contributions to the scalar mass-squared matrix.

A formula for the radiatively corrected charged Higgs mass has also been obtained.[83,89–92] The leading logarithmic piece of this formula is quite simple:

$$m_{H^\pm}^2 = m_W^2 + m_{A^0}^2 + \frac{N_c g^2}{32\pi^2 m_W^2}\left[\frac{2m_t^2 m_b^2}{s_\beta^2 c_\beta^2} - m_W^2\left(\frac{m_t^2}{s_\beta^2}+\frac{m_b^2}{c_\beta^2}\right) + \tfrac{2}{3}m_W^4\right]\ln\frac{M_{\rm SUSY}^2}{m_t^2}, \\ + \left[N_c(N_G-1)+N_G-9+15\tan^2\theta_W\right]\frac{g^2 m_W^2}{48\pi^2}\ln\frac{M_{\rm SUSY}^2}{m_W^2}, \tag{23}$$

assuming $m_{A^0} \lesssim \mathcal{O}(m_W)$. In contrast to results in the neutral Higgs sector, the leading log formula for the charged Higgs mass is not very accurate. The difference can be attributed to the absence of a leading logarithmic term in eq. (23) proportional to m_t^4. In the numerical results exhibited below, important non-leading corrections to the charged Higgs mass are also included (as described in ref. 92). However, it should be emphasized that the radiative corrections to the charged Higgs mass are generally small over nearly all of the MSSM parameter space.

Results for the radiatively corrected Higgs masses are shown in figs. 14 and 15 as a function of $\tan\beta$ for $M_{\rm SUSY} = 1$ TeV and two choices for m_{A^0} and m_t. In particular, for $m_t = m_{A^0} = 200$ GeV we see that $m_{h^0} > 97$ GeV over the entire range of $\tan\beta$ shown. More generally, for $M_{\rm SUSY} = 1$ TeV, $m_t = 200$ GeV and $m_{A^0} > m_{h^0}$, h^0 is heavier than the Z for all possible values of $\tan\beta$. In this case, the full MSSM Higgs sector would lie beyond the range of LEP-II, while h^0 would be accessible at the NLC. The radiatively corrected angle α can be used to compute the important quantity $\cos^2(\beta-\alpha)$ which governs the strength of the neutral Higgs couplings to VV and ZA^0. Results for $\cos^2(\beta-\alpha)$ as a function of m_{A^0} for two different values of m_t and $\tan\beta$ are shown (and compared to the tree-level prediction) in fig. 16. Although the rapid fall-off of the tree-level result is somewhat reduced, the basic features remain intact: (i) for $m_{A^0} \gtrsim 2m_Z$, $\sin^2(\beta-\alpha) \simeq 1$, and (ii) for $m_{A^0} \ll m_Z$ and $\tan\beta \gg 1$, $\cos^2(\beta-\alpha) \simeq 1$. These results then determine which of the following couplings, either proportional to $\sin(\beta-\alpha)$ or $\cos(\beta-\alpha)$ as indicated below, are suppressed:

$\cos(\beta-\alpha)$	$\sin(\beta-\alpha)$
$H^0W^+W^-$	$h^0W^+W^-$
H^0ZZ	h^0ZZ
ZA^0h^0	ZA^0H^0
$W^\pm H^\mp h^0$	$W^\pm H^\mp H^0$

Using the radiatively corrected values for the Higgs masses and $\cos^2(\beta-\alpha)$, one can compute the cross-sections for the various Higgs processes discussed in

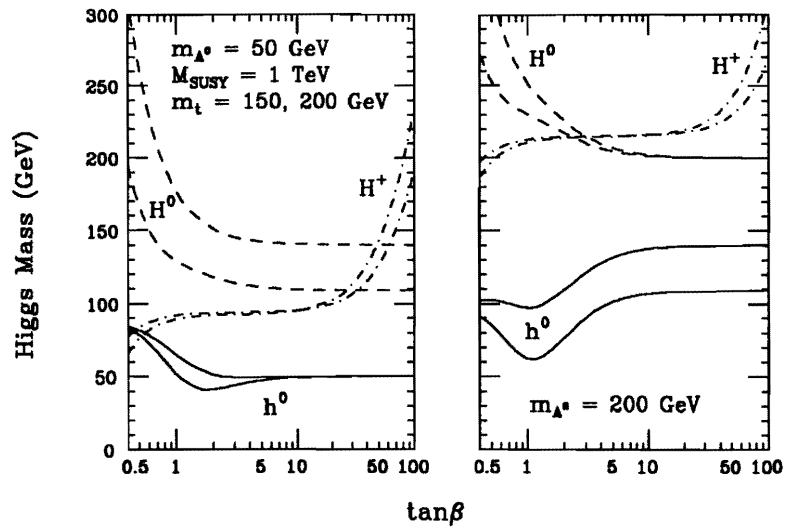

Fig. 14. The masses of h^0, H^0 and $H^\pm$ in the MSSM as a function of $\tan\beta$ for two choices of the CP-odd Higgs mass (m_{A^0}). The neutral CP-even Higgs masses are obtained from a calculation that includes the leading-logarithmic one-loop radiative corrections. The charged Higgs mass is obtained from a similar calculation, but important non-leading logarithmic effects have also been included. All supersymmetric masses are assumed to be roughly degenerate of order $M_{\rm SUSY} = 1$ TeV. The two curves for each Higgs mass shown correspond to $m_t = 150$ and 200 GeV. The larger neutral Higgs mass corresponds to the larger m_t choice. In the case of $H^\pm$, $m_{H^\pm}$ increases [decreases] with m_t for large [small] $\tan\beta$.

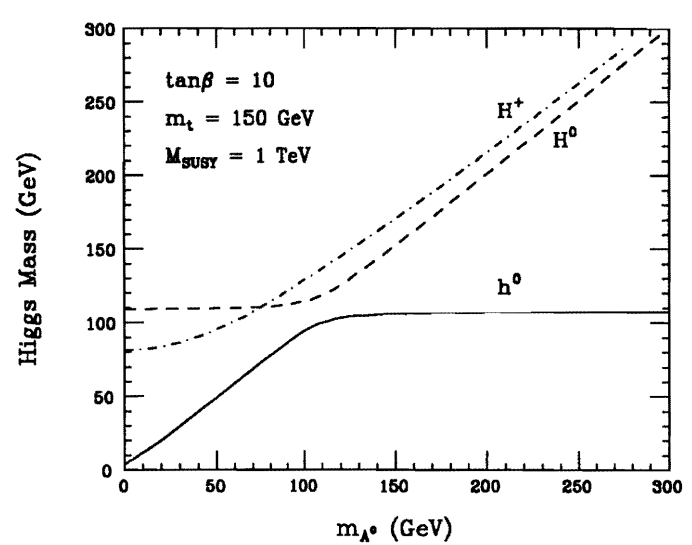

Fig. 15. The masses of h^0, H^0 and $H^\pm$ in the MSSM as a function of m_{A^0} for $\tan\beta = 10$ and $m_t = 150$ GeV. See caption to fig. 14.

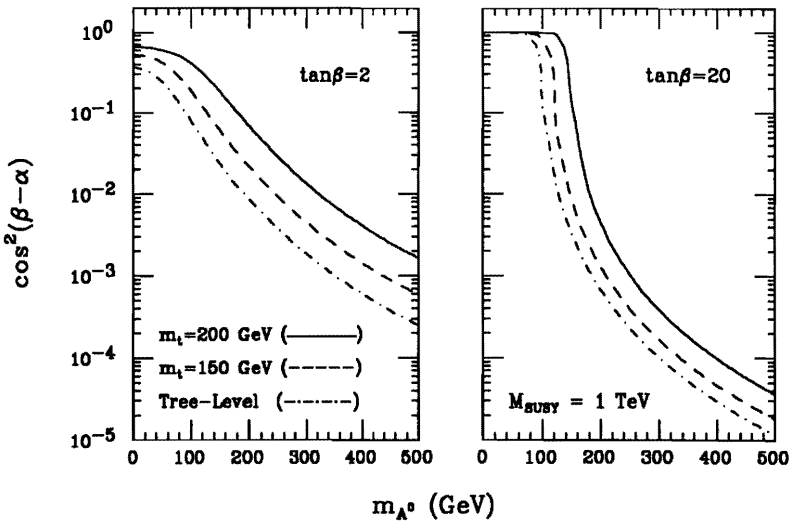

Fig. 16. The radiatively corrected angle α is obtained by diagonalizing the leading logarithmic one-loop CP-even Higgs mass matrix. Using this result, $\cos^2(\beta-\alpha)$ is obtained. Assumptions are similar to those of the previous two figures.

sections 2 and 3. These include:

$$\begin{aligned} &e^+e^- \to Zh^0, && e^+e^- \to ZH^0, \\ &e^+e^- \to h^0A^0, && e^+e^- \to H^0A^0, \\ &e^+e^- \to \nu\bar{\nu}h^0, && e^+e^- \to \nu\bar{\nu}H^0. \end{aligned} \tag{24}$$

The regions of m_{A^0}—$\tan\beta$ (or m_{A^0}—m_{h^0}) parameter space in which the above processes are observable at the NLC have been presented in the parallel sessions by Patrick Janot[93] and summarized in the plenary sessions by Fabio Zwirner[94] and J.-F. Grivaz.[95] Additional work that addresses the ability of the NLC to explore the MSSM Higgs sector can be found in ref. 96. It has already been noted above that it may not be possible to rule out the MSSM based on the non-observation of h^0 at LEP-II. However a definitive statement requires the knowledge of the value of m_t. If the top quark mass lies near its present experimental limit of 91 GeV, the effects of the radiative corrections to the Higgs masses will be no greater than a few GeV, and LEP-II could have the final word in either ruling out the MSSM or discovering the h^0.* On the other hand, if m_t is substantially larger than its present lower limit, the NLC with $\sqrt{s} \geq 300$ GeV may be required to either detect the h^0 or rule out the MSSM.

* The radiative corrections to m_{h^0} would also be less significant if $M_{\rm SUSY}$ were substantially less than 1 TeV [see fig. 13].

Although h^0 is certain to be observed at the NLC, the observation of $H^\pm$, A^0 and H^0 depends on the parameters of the MSSM. In particular, it is possible that $m_{A^0} \simeq M_{\rm SUSY}$.† In the limit of large m_{A^0}, one finds that $m_{H^\pm} \simeq m_{H^0} \simeq m_{A^0}$ and the couplings of h^0 are approximately equal to those of the minimal Higgs boson of the Standard Model. In this case, it will be very difficult to distinguish the minimal Standard Model from the MSSM on the basis of the Higgs sector alone. On the other hand, for moderate values of m_{A^0}, it is possible that some or all of the heavier Higgs states lie in a mass range accessible to the NLC. Of course, a larger center-of-mass energy at the TLC or CLIC increases the chances for exploring the complete nonminimal Higgs sector. In order to evaluate the details of the various Higgs signatures, one must compute all relevant Higgs decay mode branching ratios. Even in the absence of supersymmetric decay modes, the Higgs branching ratios are complicated functions of the MSSM parameters.[71,73,76,96,97] For example, the branching ratios for H^0 and A^0 of the MSSM as a function of Higgs mass are shown in figs. 17–18. These results incorporate one-loop leading log radiative corrections of Higgs masses and couplings as described above.

As a final example, consider the production of H^0 and A^0 in the $\gamma\gamma$ collider mode of the NLC. This work was presented by J.F. Gunion in the parallel sessions. Following the analysis previously presented in the case of the Standard Model Higgs boson at the end of section 2, we exhibit results for $\gamma\gamma \to H^0$ in fig. 19 and for $\gamma\gamma \to A^0$ in fig. 20. These results incorporate the leading log one-loop radiative corrections to the MSSM Higgs masses and couplings. The relevant background curves are also presented in each case.[46] Note that no curves are plotted for the ZZ final state. This is due to the suppression of the H^0ZZ coupling (relative to ϕ^0ZZ) and the absence of a tree-level A^0ZZ coupling, as is evident from the branching ratio curves shown in figs. 17 and 18. (The curves corresponding to ZZ and W^+W^- in fig. 18 are one-loop induced.) As a result, the detection of H^0 and A^0 in the $\gamma\gamma$ collider mode is much more problematical. It is not clear whether H^0 can be seen at all above background. However, there does appear to be a range of masses over which A^0 is detectable via its $b\bar{b}$ decay mode.

5. Summary and Open Questions

The Next e^+e^- Linear Collider (NLC) can play a key role in the elucidation of the Higgs sector. It is the definitive machine to study the intermediate Higgs mass region. It has the potential to explore many properties of the Higgs boson in detail, including the electroweak quantum numbers and the strength of the Higgs coupling to a variety of channels. The discovery of scalar couplings to a pair

† This is perhaps plausible, since $m^2_{A^0} = m^2_{12}(\tan\beta + \cot\beta)$, where m^2_{12} is a soft-supersymmetry breaking off-diagonal mass term which couples the two Higgs doublets.

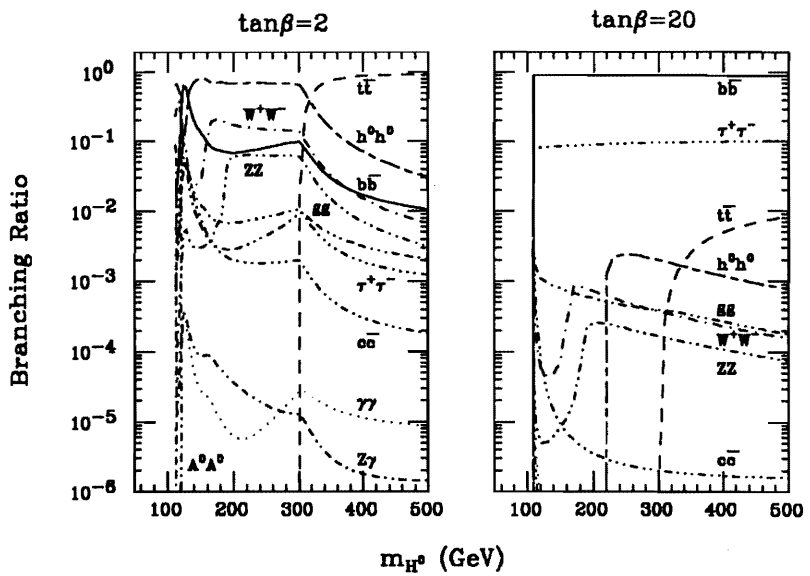

Fig. 17. Branching ratios for the H^0 computed for $m_t = 150$ GeV and for $\tan\beta = 2$ and 20. The leading logarithmic one-loop radiative corrections to MSSM Higgs masses and couplings (with $M_{\rm SUSY} = 1$ TeV) have been included. In addition, QCD corrections to Higgs decay into $Q\overline{Q}$ ($Q = c$, b and t) have been incorporated. Taken from ref. 76.

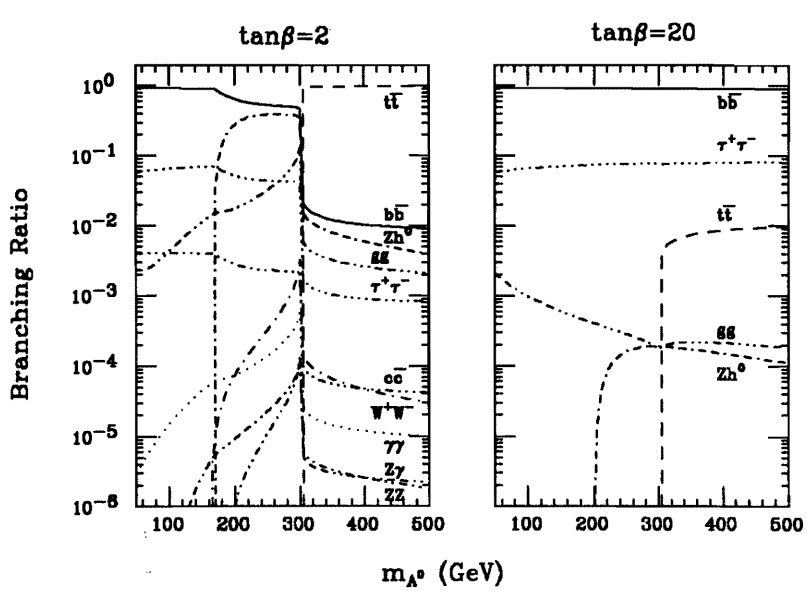

Fig. 18. Branching ratios for the A^0 computed for $m_t = 150$ GeV and for $\tan\beta = 2$ and 20. See caption to fig. 17. Taken from ref. 71.

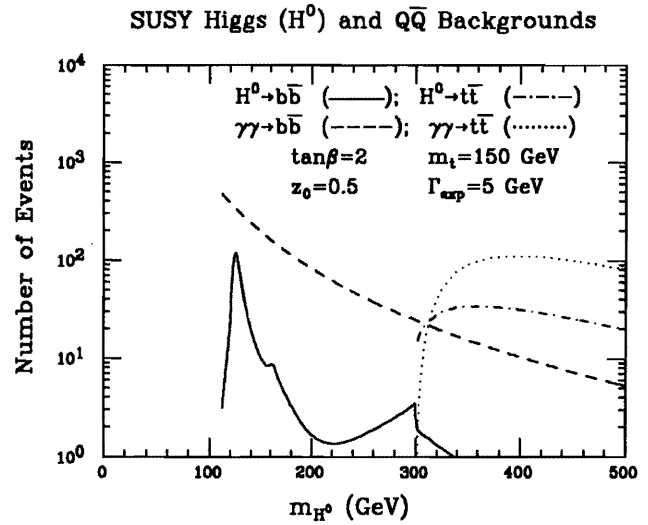

Fig. 19. As in Fig. 7, but for the heavy CP-even Higgs boson of the MSSM, H^0. Note that m_{H^0} must be greater than m_Z. Also recall that the H^0 has suppressed tree-level couplings to vector boson pairs, so that the ZZ final state is not present at a useful level. We assume that the supersymmetric partners are very heavy, so that they do not influence the $H^0\gamma\gamma$ coupling or H^0 decays.

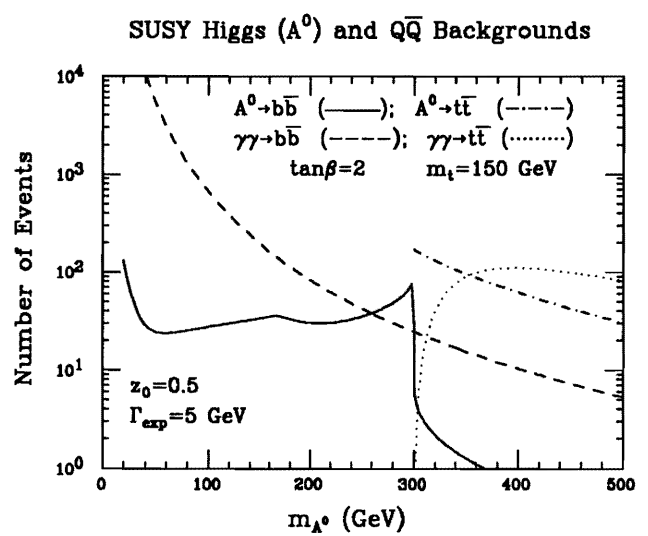

Fig. 20. As in Fig. 7, but for the CP-odd Higgs boson of the MSSM, A^0. Recall that the A^0 has no tree-level couplings to vector boson pairs, so that the ZZ final state is not present at a useful level. We assume that the supersymmetric partners are very heavy, so that they do not influence the $A^0\gamma\gamma$ coupling or A^0 decays.

of fermions (or vector bosons) whose strength is proportional to the fermion (or vector boson) mass would provide strong evidence for the Higgs boson. A detailed analysis of these couplings could either confirm or rule out the predictions of the minimal Standard Model and/or its supersymmetric extension. The NLC is ideally suited for exploring the physics of a nonminimal Higgs sector. In particular, it may provide the crucial test of the minimal supersymmetric model (MSSM) based on the properties of the MSSM constrained Higgs sector. If the lightest CP-even Higgs boson is not discovered at LEP-II, it must be produced at the NLC. Other heavier Higgs states may or may not be produced at the NLC depending on their masses. Higher center-of-mass energies may be required for a complete exploration of the Higgs sector.

I shall conclude with some open questions for future workshops on Higgs hunting at e^+e^- linear colliders.

1. How should experiments be designed to measure the following quantities:
   - CP-violation in the Higgs sector (if it exists)
   - $\tan\beta$ in a two-doublet Higgs model
   - The Higgs mixing angle α in a two-doublet Higgs model
   - Three-Higgs-boson couplings
   - Four-Higgs-boson couplings
   - Possible deviations from the minimal Higgs sector of the Standard Model, if no additional Higgs states beyond h^0 are detected.
   - Possible deviations from the Higgs sector of the MSSM.
2. What are the phenomenological consequences of other paths along the Higgs Hunter's Flow Chart? Despite my personal enthusiasm for the MSSM, nature could very well take an alternative path.
3. In the context of the MSSM, what are the phenomenological consequences of heavy Higgs bosons with supersymmetric decay modes? Presumably, if the MSSM is correct, various details of the supersymmetric spectrum will have already been determined at the SSC and LHC. In addition, if the Higgs bosons at an e^+e^- supercollider decay into chargino and/or neutralino pairs, then these supersymmetric particles can also be directly produced.[24,95,98] In this case, the study of Higgs bosons will become another branch of supersymmetric phenomenology.
4. Looking beyond the NLC, if the electroweak symmetry breaking sector is not weakly coupled, then one may have to seriously examine the various strong coupling scenarios (*e.g.*, technicolor, composite Higgs bosons, *etc.*) that have been put forward. A detailed study of vector boson self interactions at the highest possible energies (of order 1 TeV and greater) will be necessary to unlock the mysteries of the origins of electroweak symmetry breaking.[16,17]

In the energy frontier, the hadron supercolliders have certainly taken the lead. Consequently, the SSC and LHC will probably provide us with the first clues in the exploration of the TeV scale and the search for the origins of electroweak symmetry breaking. However, it is quite likely that a complete and definitive understanding of these important questions will emerge only after results are obtained from experiments at future e^+e^- supercolliders.

Acknowledgments

I would like to express my appreciation to my collaborators Marco Diaz, Jack Gunion and Ralf Hempfling for their contributions to some of the topics discussed in this report. I am also grateful to Barbara Mele and Fabio Zwirner for a number of useful conversations during my stay in Saariselkä. Finally, I thank Bernd Kniehl for providing me the TOPDRAW files to figs. 8 and 9, and permitting their reproduction in this paper. This work was supported in part by the U.S. Department of Energy.

References

1. F. Abe *et al.* [CDF Collaboration], *Phys. Rev. Lett.* **68** (1992) 447.
2. The LEP Collaborations: ALEPH, DELPHI, L3, and OPAL, *Phys. Lett.* **B276** (1992) 247; J. Ellis, G.L. Fogli and E. Lisi, *Phys. Lett.* **B274** (1992) 456; P. Renton, Oxford preprint OUNP-91-30 (1991); D. Schaile, CERN-PPE/91-187 (1991).
3. P. Langacker, U. Penn preprint UPR-0492T (1992), invited talk presented at the International Workshop on Electroweak Physics Beyond the Standard Model, Valencia, Spain, September, 1991; contributions to the 1992 Review of Particle Properties, *Phys. Rev.* **D45** Part 2 (June, 1992).
4. See, *e.g.*, L. Susskind, *Phys. Rep.* **104** (1984) 181.
5. E. Farhi and L. Susskind, *Phys. Rep.* **74** (1981) 277; R.K. Kaul, *Rev. Mod. Phys.* **55** (1983) 449.
6. G. 't Hooft, in *Recent Developments in Gauge Theories, Proceedings of the NATO Advanced Summer Institute*, Cargese, 1979, edited by G. 't Hooft *et al.* (Plenum, New York, 1980) p. 135.
7. E. Witten, *Nucl. Phys.* **B188** (1981) 513; S. Dimopoulos and H. Georgi, *Nucl. Phys.* **B193** (1981) 150; N. Sakai, *Z. Phys.* **C11** (1981) 153.

8. H.E. Haber, in *Testing the Standard Model*, Proceedings of the 1990 Theoretical Advanced Study Institute in Elementary Particle Physics, edited by M. Cvetič and Paul Langacker (World Scientific, Singapore, 1991) pp. 340–475.

9. J.F. Gunion, H.E. Haber, G. Kane and S. Dawson, *The Higgs Hunter's Guide* (Addison-Wesley Publishing Company, Reading, MA, 1990).

10. K. Inoue, A. Komatsu and S. Takeshita, *Prog. Theor. Phys.* **67** (1982) 927 [E: **70** (1983) 330]; **71** (1984) 413; R. Flores and M. Sher *Ann. Phys. (NY)* **148** (1983) 95.

11. J.F. Gunion and H.E. Haber, *Nucl. Phys.* **B272** (1986) 1.

12. J.F. Gunion and H.E. Haber, *Nucl. Phys.* **B278** (1986) 449.

13. N. Cabibbo, L. Maiani, G. Parisi, R. Petronzio, *Nucl. Phys.* **B158** (1979) 295.

14. J. Kuti, L. Lin, and Y. Shen, *Phys. Rev. Lett.* **61** (1988) 678; M. Luscher and P. Weisz, *Nucl. Phys.* **B290** (1987) 25; **B295** (1988) 65; **B318** (1989) 705.

15. U.M. Heller, H. Neuberger and P. Vranas, SCRI preprint, FSU-SCRI-91-94 (1991).

16. K. Hikasa, KEK-TH-319 (1992), in These Proceedings.

17. M.S. Chanowitz, *"Physics at TeV e^+e^- Linear Colliders"*, invited talk given at the Second KEK Topical Conference on e^+e^- Collision Physics, KEK, Tsukuba, Japan, 26–29 November, 1991, LBL-31651 (1992).

18. S. Dawson and G. Valencia, *Nucl. Phys.* **B352** (1991) 27; A. Dobado and M.J. Herrero, *Phys. Lett.* **B233** (1989) 505; A. Dobado, M.J. Herrero and T.N. Troung, *Phys. Lett.* **B235** (1990) 129; A. Dobado, D. Espriu, and M.J. Herrero, *Phys. Lett.* **B255** (1991) 405.

19. B.W. Lee, *Proceedings of the XVI International Conference on High Energy Physics*, Batavia, IL (1972), ed. J.D. Jackson, A. Roberts and R. Donaldson, Vol. 4, p. 249; D.A. Ross and M. Veltman *Nucl. Phys.* **B95** (1975) 135.

20. H.-S. Tsao, in *Proceedings of the 1980 Guangzhou Conference on Theoretical Particle Physics*, edited by H. Ning and T. Hung-yuan, (Science Press, Beijing, 1980) p. 1240.

21. T.D. Lee, *Phys. Rev.* **D8** (1973) 1226; *Phys. Rep.* **9** (1974) 143; S. Weinberg, *Phys. Rev. Lett.* **37** (1976) 657; *Phys. Rev.* **D42** (1990) 860; J. Liu and L. Wolfenstein, *Nucl. Phys.* **B289** (1987) 1.

22. H.P. Nilles, *Phys. Rep.* **110** (1984) 1; H.E. Haber and G.L. Kane, *Phys. Rep.* **117** (1985) 75; R. Barbieri, *Riv. Nuovo Cimento* **11** (1988) 1.

23. J. Ellis, J.F. Gunion, H.E. Haber, L. Roszkowski, and F. Zwirner, *Phys. Rev.* **D39** (1989) 844.

24. C. Ahn *et al.*, SLAC-Report-329, (May 1988).

25. See the reports by G. Altarelli, D. Froidevaux, B. Mele, and F. Richard, in *Proceedings of the Workshop on Physics at Future Accelerators*, La Thuile, vols. 1 and 2, edited by J.H. Mulvey, CERN 87-07 (1987).

26. M. Lindner, *Z. Phys.* **C31** (1986) 295; see also §2.5 of ref. 9.

27. D. Decamp *et al.* (ALEPH Collaboration) *Phys. Lett.* **B245** (1990) 289; **B246** (1990) 306; P. Abreu *et al.* (DELPHI Collaboration), CERN-PPE-91-132 (1991), to appear in *Nucl. Phys. B*; *Z. Phys.* **C51** (1991) 25; B. Adeva *et al.* (L3 Collaboration) *Phys. Lett.* **B248** (1990) 203; **B252** (1990) 518; M. Akrawy *et al.* (OPAL Collaboration) *Phys. Lett.* **B251** (1990) 211; **B253** (1991) 511.

28. F. Merrit, invited talk at the 1992 Aspen Winter Conference on Elementary Particle Physics, January 12-19, 1992.

29. J. Hilgart, M. Mermikides, S. Ritz, S.L. Wu and G. Zobernig, *Z. Phys.* **C35** (1987) 347; K.J.F. Gaemers and N. de Groot, *Z. Phys.* **C49** (1991) 267.

30. Z. Kunszt and W.J. Stirling, *Phys. Lett.* **B242** (1990) 507; N. Brown, *Z. Phys.* **C49** (1991) 657; V. Barger, R.J.N. Phillips and K. Whisnant, *Phys. Rev.* **D43** (1991) 1110; D.J. Summers, *Phys. Lett.* **B274** (1992) 209.

31. G. Altarelli, *"Physics at Supercolliders: Search for the Higgs"*, invited talk given at the International Workshop on Electroweak Physics Beyond the Standard Model, Valencia, Spain, 2–5 October 1991, CERN-TH 6317/91 (1991).

32. J.F. Gunion, preprint UCD-91-9, to appear in *Proceedings of the 'Workshop in High Energy Physics Phenomenology — II'*, Calcutta (January, 1991).

33. J.F. Gunion, G.L. Kane *et al.*, *Overview and Recent Progress in Higgs Boson Physics at the SSC*, to appear in *Proceedings of the 1990 DPF Summer Study on High Energy Physics*, Snowmass, CO (1990); Z. Kunszt and W.J. Stirling, in *Proceedings of the Large Hadron Collider Workshop*, Aachen, October 1990, edited by G. Jarlskog and D. Rein, CERN 90-10, ECFA 90-133, Vol.II, p. 428; D. Froidevaux, *ibid*, p. 444.

34. J.F. Gunion, G.L. Kane, and J. Wudka, *Nucl. Phys.* **B299** (1988) 231; R. Kleiss, Z. Kunszt and W.J. Stirling, *Phys. Lett.* **B253** (1991) 269; J.F. Gunion, *Phys. Lett.* **B261** (1991) 510; W.J. Marciano and F.E. Paige, *Phys. Rev. Lett.* **66** (1991) 2433; A. Ballestrero and E. Maina, *Phys. Lett.* **B268** (1991) 437; Z. Kunszt, Z. Trócsányi and W.J. Stirling, *Phys. Lett.* **B271** (1991) 247; R.K. Ellis, I. Hinchliffe, M. Soldate and J.J. van der Bij, *Nucl. Phys.* **B297** (1988) 221.

35. T.L. Barklow, SLAC-PUB-3564 (1990), to appear in *The Proceedings of the 1990 DPF Summer Study on High Energy Physics*, Snowmass, CO, June 25-July 13, 1990; V. Telnov, in These Proceedings.

36. D.L. Borden, D.A. Bauer, and D.O. Caldwell, SLAC-PUB-5715 (1992).

37. G. Altarelli, B. Mele, and F. Pitolli, *Nucl. Phys.* **B287** (1987) 205.

38. P.R. Burchat, D.L. Burke, and A. Petersen, *Phys. Rev.* **D38** (1988) 2735 [E: **D39** (1989) 3515.

39. V. Barger, K. Cheung, B.A. Kniehl, and R.J.N. Phillips, MAD/PH/610 (1992).

40. S. Dawson and J.L. Rosner, *Phys. Lett.* **B148** (1984) 497; G. Altarelli and E. Franco, *Mod. Phys. Lett.* **A1** (1986) 517; A. Tofighi-Niaki and J.F. Gunion, *Phys. Rev.* **D36** (1987) 2671; **D38** (1988) 1433; G.L. Kane and J. Scanio, *Nucl. Phys.* **B291** (1987) 221.

41. B. Mele, presented in the parallel sessions of this Workshop.

42. A. Djouadi, J. Kalinowski and P.M. Zerwas, DESY-91-104 (1991).

43. J.A. Grifols and R. Pascual, *Z. Phys.* **C6** (1980) 353; M. Hayashi and K. Katsuura, *Lett. Nuovo Cim.* **44** (1985) 235.

44. J.F. Gunion, L. Roszkowski, A. Turski, H.E. Haber, G. Gamberini, B. Kayser, S.F. Novaes, F. Olness, and J. Wudka, *Phys. Rev.* **D38** (1988) 3444.

45. J.F. Gunion and H.E. Haber, SCIPP-90/22 (1990), to appear in *The Proceedings of the 1990 DPF Summer Study on High Energy Physics*, Snowmass, CO, June 25-July 13, 1990.

46. J.F. Gunion and H.E. Haber, preprint in preparation.

47. V. Barger, T. Han and R.J.N. Phillips, *Phys. Rev.* **D38** (1988) 2766; V. Barger and T. Han, *Mod. Phys. Lett.* **A5** (1990) 667.

48. V. Barger, T. Han and A. Stange, *Phys. Rev.* **D42** (1990) 777.

49. B.A. Kniehl, *Nucl. Phys.* **B352** (1991) 1.

50. B.A. Kniehl, *Nucl. Phys.* **B357** (1991) 439.

51. J. Fleischer and F. Jegerlehner, *Nucl. Phys.* **B228** (1983) 1.

52. S. Dawson and H.E. Haber, *Phys. Rev.* **D44** (1991) 53.

53. W.F.L. Hollik, *Fortschr. Phys.* **38** (1990) 165.

54. J. Fleischer and F. Jegerlehner, *Nucl. Phys.* **B216** (1983) 469; F. Jegerlehner, in *Proceedings of the Topical Conference on Radiative Corrections in $SU(2)_L \times U(1)$*, Trieste, Italy, 1983, edited by B.W. Lynn and J.F. Wheater (World Scientific, Singapore, 1984), p. 237.

55. B.A. Kniehl, DESY-91-128 (1991).

56. P. Langacker and M. Luo, *Phys. Rev.* **D44** (1991) 817; T.G. Rizzo, *Mod. Phys. Lett.* **A6** (1991) 1961.

57. See Chapter 4 of ref. 9 and references therein.

58. H.E. Haber and Y. Nir, *Nucl. Phys.* **B335** (1990) 363.

59. J.F. Gunion, H.E. Haber and J. Wudka, *Phys. Rev.* **D43** (1991) 904.

60. S. Glashow and S. Weinberg, *Phys. Rev.* **D15** (1977) 1958.

61. See §4.1 of ref. 9 and the references therein.

62. S. Komamiya, *Phys. Rev.* **D38** (1988) 2158.

63. M. Drees and D.P. Roy, *Phys. Lett.* **B269** (1991) 155.

64. J. Alexander, D.L. Burke, C. Jung, S. Komamiya, and P. Burchat, in *Proceedings of the Summer Study on High Energy Physics in the 1990s*, June 27—July 15, 1988, Snowmass, CO, edited by S. Jensen (World Scientific, Singapore, 1989) p. 135.

65. J.F. Gunion and H.E. Haber, *Nucl. Phys.* **B307** (1988) 445.

66. G.J. Gounaris and A. Nicolaidis, *Phys. Lett.* **102B** (1981) 144; J.R. Dell'Aquila and C.A. Nelson, *Phys. Rev.* **D33** (1986) 80, 93; *Nucl. Phys.* **B320** (1989) 61, 86.

67. J.F. Gunion, H.E. Haber, S. Komamiya, H. Yamamoto, and A. Barbaro-Galtieri, in *Proceedings of the 1987 Berkeley Workshop on Experiments, Detectors and Experimental Areas for the Supercollider*, edited by R. Donaldson and M. Gilchriese (World Scientific, Singapore, 1988), p. 110.

68. R.M. Barnett, I. Hinchliffe, J.F. Gunion, B. Hubbard, H.E. Haber, and H.-J. Trost, ANL-HEP-TR-90-86 (1990).

69. R.M. Barnett *et al.*, ANL-HEP-CP-90-98, to appear in *The Proceedings of the 1990 DPF Summer Study on High Energy Physics*, Snowmass, CO, June 25-July 13, 1990.

70. D.P. Roy, CERN-TH-6247-91 (1991); R.M. Godbole and D.P. Roy, *Phys. Rev.* **D43** (1991) 3641.

71. J.F. Gunion, H.E. Haber and C. Kao, UCD-91-32 and SCIPP-91/44 (1991).

72. J.F. Gunion and L.H. Orr, UCD-91-15 (1991).

73. V. Barger, M.S. Berger, A.L. Stange, and R.J.N. Phillips, MAD/PH/680 (1991).

74. Z. Kunszt and F. Zwirner, in *Proceedings of the Large Hadron Collider Workshop*, Vol. II, edited by G. Jarlskog and D. Rein, CERN 90-10 (1990), p. 578; ETH-TH/91-7 (1991).

75. H. Baer, M. Bisset, C. Kao and X. Tata, FSU-HEP-911104 (1991).

76. J.F. Gunion, R. Bork, H.E. Haber and A. Seiden, UCD-91-29 and SCIPP-91/34 (1991), to be published in *Phys. Rev. D.*

77. See §4.2 of ref. 9 and the references therein.

78. M. Berger, *Phys. Rev.* **D41** (1990) 225.

79. H.E. Haber and R. Hempfling, *Phys. Rev. Lett.* **66** (1991) 1815.

80. Y. Okada, M. Yamaguchi and T. Yanagida, *Prog. Theor. Phys.* **85** (1991) 1; *Phys. Lett.* **B262** (1991) 54; J. Ellis, G. Ridolfi and F. Zwirner, *Phys. Lett.* **B257** (1991) 83; **B262** (1991) 477; R. Barbieri, M. Frigeni, and F. Caravaglios, *Phys. Lett.* **B258** (1991) 167.

81. R. Barbieri and M. Frigeni, *Phys. Lett.* **B258** (1991) 395; A. Yamada, *Phys. Lett.* **B263** (1991) 233.

82. J.R. Espinosa and M. Quiros, *Phys. Lett.* **B267** (1991) 27.

83. P.H. Chankowski, S. Pokorski and J. Rosiek, *Phys. Lett.* **B274**, 191 (1992).

84. H.E. Haber and R. Hempfling, SCIPP-91/33 (1992).

85. D.M. Pierce, A. Papadopoulos, and S. Johnson, LBL-31416 (1991).

86. K. Sasaki, M. Carena and C.E.M. Wagner, MPI-Ph/91-109 (1991).

87. A. Brignole, CERN-TH-6366/92 (1992).

88. M.A. Diaz and H.E. Haber, SCIPP-91/13 (1992).

89. J.F. Gunion and A. Turski, *Phys. Rev.* **D39** (1989) 2701; **D40** (1989) 2333.

90. A. Brignole, J. Ellis, G. Ridolfi and F. Zwirner, *Phys. Lett.* **B271** (1991) 123; [E: **B273** (1991) 550].

91. A. Brignole, preprint DFPD/91/TH/28 (1991).

92. M.A. Diaz and H.E. Haber, SCIPP-91/14 (1991), to be published in *Phys. Rev. D.*

93. P. Janot, LAL 91-61 (1991), in These Proceedings.

94. F. Zwirner, CERN-TH-6357 (1991), in These Proceedings.

95. J.-F. Grivaz, LAL 91-63 (1991), in These Proceedings.

96. A. Yamada, preprint UT-Komaba 92-1 (1992).

97. H.E. Haber, R. Hempfling and Y. Nir, SCIPP-91/40 and WIS-92/5/Feb-PH (1992).

98. H. Baer, A. Bartl, D. Karatas, W. Majerotto and X. Tata, *Int. J. Mod. Phys.* **A4** (1989) 4111; C. Dionisi and M. Dittmar, in *Proceedings of the Workshop on Physics at Future Accelerators*, La Thuile, vol. 2, edited by J.H. Mulvey, CERN 87-07 (1987), p. 149.